Expanding the current knowledge and biotechnological applications of the oxygen-independent *ortho*-phthalate degradation pathway

David Sanz, José L. García and Eduardo Díaz *

Department of Microbial and Plant Biotechnology, Centro de Investigaciones Biológicas Margarita Salas-CSIC, Ramiro Maeztu 9, 28040 Madrid, Spain

***Corresponding author:**

Eduardo Díaz

Environmental Microbiology Group, Department of Microbial and Plant Biotechnology, Centro de Investigaciones Biológicas Margarita Salas-CSIC, Ramiro Maeztu 9, 28040 Madrid, Spain

Tel. (+34) 918373112

Fax: (+34) 915360432

Email: ediaz@cib.csic.es

Running title: The *o*-phthalate pht peripheral pathway

Keywords: *o*-phthalate, *Azoarcus, Cupriavidus*, biodegradation, transport, polyhydroxybutyrate

Originality-Significance Statement

Bacteria adapt rapidly their catabolic abilities to benefit from certain substrates, such as *ortho*-phthalate (PA), that have recently been introduced into the ecosystem by humans. We show here that in addition to the enzymatic repertoire, the recruitment of an active transport system is mandatory for PA uptake and degradation through the anaerobic pht pathway. The construction of a fully functional *pht* cassette combining both catabolic and transport genes revealed the unexpected finding that it allows PA degradation also under aerobic conditions when combined with a functional aerobic hybrid benzoate central pathway (box pathway) in the host cell. The acquired knowledge on the pht pathway has allowed us to engineer recombinant bacteria that can be useful to recycling at industrial scale PA derived from plastics towards the production of sustainable bioplastics.

Summary

***ortho*-Phthalate derives from industrially produced phthalate esters which are massively used as plasticizers and constitute major emerging environmental pollutants. The pht pathway for the anaerobic bacterial biodegradation of *o*-phthalate involves its activation to phthaloyl-CoA followed by decarboxylation to benzoyl-CoA. Here we have explored further the pht peripheral pathway in denitrifying bacteria and shown that it requires also an active transport system for *o*-phthalate uptake that belongs to the poorly characterized class of TAXI-TRAP transporters. The construction of a fully functional *pht* cassette combining both catabolic and transport genes allowed to expand the *o*-phthalate degradation ecological trait to heterologous hosts. Unexpectedly, the *pht* cassette also allowed the aerobic conversion of *o*-phthalate to benzoyl-CoA when coupled to a functional box central pathway. Hence, the pht pathway may constitute an evolutionary acquisition for *o*-phthalate degradation by bacteria that thrive either in anoxic environments, or in environments that face oxygen limitations and that rely on benzoyl-CoA, rather than on catecholic central intermediates, for the aerobic catabolism of aromatic compounds. Finally, the recombinant *pht* cassette was used both to screen for functional aerobic box pathways in bacteria, and to engineer recombinant biocatalysts for *o*-phthalate bioconversion into sustainable bioplastics, e.g., polyhydroxybutyrate, in plastic recycling industrial processes.**

Introduction

Phthalic acids are benzoic acids with one additional carboxylic group in either *ortho* (*o*-phthalate, PA), *meta* (isophthalate) or *para* (terephthalate) position. Although these compounds are generated as intermediates during the bacterial degradation of polycyclic aromatic hydrocarbons found in fossil fuels, the main source of phthalic acids is the chemical industry (Junghare *et al*., 2016). Phthalic acids are produced massively as essential constituents of plastics, either as part of the polymeric structure, e.g., terephthalate in polyethylene terephthalate (PET) plastic, or as non-covalently bound dissolved additives (softeners or plasticizers) (Gao and Wen, 2016). Most synthetic plasticizers are di-esters of PA (called phthalates) and they are classified as xenobiotics produced industrially only since the 1960s (Benjamin *et al*., 2015). As PA esters are not covalently bound to the plastic, they can easily diffuse out of the polymer itself, leading to contamination in nearly every environment. PA esters are one of the most frequently detected emerging organic contaminants in the environment (Gao and Wen, 2016), and they have been listed as major man-made priority pollutants due to their hepatotoxic, teratogenic, carcinogenic and endocrine disrupting (anti-androgenic) properties (Annamalai and Namasivayam, 2015). Hence, it becomes urgent to remove phthalates from the environment effectively and economically. On the other hand, and within the current strategies for plastic recycling as a sustainable plastic waste management, the treatment of the PA esters constitutes a major challenge (Brandon and Criddle, 2019; Boll *et al.*, 2020).

Compared to abiotic degradation, microbial degradation of PA esters is a more efficient, cost-effective and environmental-friendly strategy in the ecosystem. In most

cases, biodegradation is initiated by non-specific esterases that release the free PA moiety and the side chain alcohols (Keyser *et al.*, 1976; Eaton and Ribbons, 1982; Liang *et al.*, 2008). The latter are being utilized by microorganisms while PA is quite resistant and persists in the environment (Gao and Wen, 2016). However, certain microorganisms can mineralize PA, as well as the other two phthalate isomers, under aerobic conditions. In all cases, the three phthalate isomers are converted to a dihydroxybenzoic acid by the action of ring-hydroxylating dioxygenases and subsequent decarboxylation. Protocatechuate, in most cases, or 2,3-dihydroxybenzoate are then attacked by ring-cleavage dioxygenases and converted to central intermediates either via the *ortho*- or *meta*-cleavage pathways (Ribbons and Evans, 1960; Keyser *et al.*, 1976; Eaton and Ribbons, 1982; Boll *et al.*, 2020; Kasai *et al.*, 2019).

In contrast to the well-studied aerobic biodegradation of PA, anaerobic biodegradation of PA was reported later in the literature (Nozawa and Maruyama, 1988). Only very recently some studies based on differential proteomics and *in vitro* enzyme assays, allowed the identification and characterization of the genes (hereafter named as *pht*) and enzymes involved in the anaerobic peripheral pathway for the conversion of PA to benzoyl-CoA (Boll *et al*., 2020), which is further degraded through the anaerobic benzoyl-CoA central pathway (*bzd* genes) (Carmona *et al.*, 2009) (Fig. 1A). The pht peripheral pathway has been studied in closely related denitrifying β-proteobacteria, such as *Azoarcus* sp. PA01 (Junghare *et al*., 2016), *Thauera chlorobenzoica* 3CB-1, *Aromatoleum aromaticum* EbN1 and *Azoarcus evansii* KB740 (recently reclassified within the *Aromatoleum* genus; (Rabus *et al.*, 2019)) (Ebenau-Jehle *et al*., 2017), and in an obligate anaerobic sulfate-reducing δ–proteobacterium,

Desulfosarcina cetonica (Geiger *et al*., 2019). Whereas in denitrifyers the PA is first activated to phthaloyl-CoA by a heterodimeric class III succinyl-CoA-dependent PA CoA transferase (SPT) (Junghare *et al*., 2016; Mergelsberg *et al.*, 2018) (Fig. 1A), in sulfate-reducing bacteria the activation is carried out by an ATP-dependent PA CoA ligase (Geiger *et al*., 2019). Nevertheless, both in denitrifying and sulfate-reducing bacteria, *o*-phthaloyl-CoA is subsequently decarboxylated to benzoyl-CoA by a phthaloyl-CoA decarboxylase (PCD). PCD belongs to the UbiD enzyme family of (de)carboxylases that contain a prenylated flavin adenosine mononucleotide (prFMN) cofactor generated by an associated UbiX-type prenyltransferase (Fig. 1A) (Junghare *et al.*, 2016; Mergelsberg *et al*., 2017; Geiger *et al*., 2019; Marshall *et al.*, 2019). A similar biochemical strategy has been recently described for the anaerobic biodegradation of isophthalate in the fermenting bacterium *Syntrophorhabdus aromaticivorans* (Junghare *et al*., 2019).

All PA-induced *pht* gene clusters described so far contain at least four genes (three genes in obligate anaerobes) encoding the enzymes SPT (*phtSaSb*), PCD (*phtDa*) and its associated FMN prenyltransferase (*phtDb*), as well the two additional genes *phtTaTb* proposed to encode a PA transporter (Boll *et al*., 2020) but whose implication in PA transport has not been demonstrated so far (Fig. 1).

In the aerobic degradation of PA, uptake into bacterial cells appears to require an active transport system, i.e., either mono-component permeases of the major facilitator superfamily (MFS) of transporters or multicomponent solute-binding protein (SBP) dependent transport systems that rely on a periplasmic SBP protein which interacts with the substrate with high affinity (Chang *et al.,* 2009; Hara *et al.,* 2010; Fukuhara *et al.,* 2010; Hosaka *et al*., 2013), rather than its passive diffusion across the

inner membrane which only may work at low external pH when the carboxylic groups are protonated. However, there is no experimental demonstration that an active uptake is also essential for anaerobic PA degradation.

The initial aim of this work was to experimentally demonstrate for the first time that PA uptake in denitrifying bacteria requires an SBP-dependent secondary transporter (PhtTaTb) that becomes essential for anaerobic PA degradation through the peripheral pht pathway. The construction of a fully functional cassette to confer PA degradation to heterologous hosts has allowed us to discover that unexpectedly the pht pathway also allows the aerobic conversion of PA to benzoyl-CoA opening a new view about the biological significance and evolution of this route primarily classified as a strict anaerobic pathway. Finally, using the newly acquired knowledge on the pht pathway we have been able of engineering novel recombinant organisms to channel the degradation of PA, a major feedstock from plastic recycling processes, towards the industrial production of more sustainable bioplastics.

Results and Discussion

Anaerobic PA degradation requires an active uptake system

The peripheral pht pathway for the anaerobic degradation of PA in certain denitrifying bacteria involves only two enzymatic steps catalyzed by the SPT and PCD enzymes (Fig. 1A) (Junghare *et al.*, 2016; Mergelsberg *et al.*, 2017; Mergelsberg *et al*., 2018). To check whether the expression of the four *phtDbDaSbSa* catabolic genes (Fig. 1B) would confer to other denitrifying bacteria the ability to use PA as sole carbon an energy source, we cloned these genes from *A. aromaticum* EbN1 strain and expressed them in *Escherichia coli* from a pIZ1016 broad-host range plasmid (Table 1) under the control

of the *Ptac/lacI*^{q} regulatory couple. The resulting pIZPHT plasmid (Table 1) was then introduced into *Azoarcus* sp. CIB, an anaerobic benzoate/benzoyl-CoA degrader that lacks the *pht* genes and, hence, is naturally unable to degrade PA (Martín-Moldes *et al.*, 2015). Interestingly, *Azoarcus* sp. CIB (pIZPHT) was unable to grow on PA as sole carbon source, even after the induction of the *pht* genes by the addition of IPTG to the cultures. This result suggested that the peripheral pht pathway for PA degradation may involve functions other than those strictly responsible for its activation/decarboxylation to benzoyl-CoA. In this sense, it is known that the aerobic degradation of phthalates requires their uptake into the bacterial cell through a specific transport system (Chang *et al.,* 2009; Hara *et al.,* 2010; Fukuhara *et al.,* 2010; Hosaka *et al*., 2013), and all the PA-induced *pht* clusters reported so far contain a couple of genes (*phtTaTb*) predicted to encode an SBP-dependent secondary transporter (Boll *et al*., 2020) (Fig. 1B). Moreover, additional genes located near the *pht* genes in the genomes of some denitrifying bacteria encode a putative three-component primary ATP-dependent (ABC) transporter that could also be involved in PA uptake (Junghare *et al*., 2016; Ebenau-Jehle *et al.,* 2017; Boll *et al.*, 2020). Therefore, all these observations suggested that an active PA uptake could be essential for the anaerobic degradation of PA through the pht pathway.

To get some insights into PA transport in denitrifying bacteria that naturally express the pht peripheral pathway, we used *A. evansii* as model system. Cells grown anaerobically on MC medium containing 3 mM benzoate (control condition) or 3 mM PA, were incubated with 25 μM [^{14}C]-PA, and a time-course of the amount of [^{14}C]-PA incorporated into the cells was determined. Whereas cells grown on PA showed uptake of this aromatic acid (uptake rate of about 670 pmol min^{-1} mg protein^{-1}) cells

184 grown on benzoate did not show [^{14}C]-PA uptake (Fig. 2A). This result suggested that a
185 specific PA transporter is induced when cells grow on this aromatic compound.
186 To determine whether the uptake of PA requires an active transport system, *A.*
187 *evansii* cells grown on PA were exposed to 2,4-dinitrophenol (DNP), an ionophore
188 which disrupts the proton motive force, or to 1,3-dicyclohexylcarbodiimide (DCCD),
189 which blocks ATP synthesis by acting on the ATPase complex (Chae and Zylstra, 2006),
190 before the transport assay was performed. Whereas cells treated with DCCD retained
191 the PA transport capacity, cells exposed to DNP lacked completely the ability to
192 transport [^{14}C]-PA (Fig. 2B). Thus, these results indicate that PA uptake in *A. evansii*
193 cells requires an active transport system that is mainly dependent on the proton
194 motive force rather than on the ATP pool, hence suggesting the involvement of an SBP-
195 dependent secondary transporter instead of a primary ABC-type transport mechanism
196 (Mulligan *et al.,* 2011).
197
198 *Engineering a fully functional pht pathway*
199 Once it was shown that an active secondary transport system is induced when cells
200 grow anaerobically on PA, we engineered a new recombinant *pht* cassette containing
201 the four *pht* catabolic genes and the closely associated *phtTaTb* genes, under control
202 of the *Ptac/lacI*^{q} regulatory couple generating the broad-host range pIZPHTRAP
203 plasmid (Fig. 3A, Table 1). *Azoarcus* sp. CIB (pIZPHTRAP) acquired the ability to use PA
204 as sole carbon and energy source under anaerobic conditions (Fig. 3B), hence
205 demonstrating that both catabolic genes (*phtDbDaSbSa*) and the putative transport
206 genes (*phtTaTb*) are essential for the anaerobic degradation of PA via benzoyl-CoA.

We show here that an active transport system is essential for the peripheral pht pathway to metabolize PA via CoA-derived intermediates. Although transport genes are usually found associated to clusters for anaerobic degradation of polar dissociated aromatic compounds, e.g., aromatic acids (Egland *et al*., 1997; Carmona *et al*., 2009; Trautwein *et al.*, 2012; Juárez *et al.*, 2013), and some SBPs have been studied *in vitro* (Pietri *et al.*, 2012; Salmon *et al*., 2013) nobody had demonstrated their physiological role so far. Thus, our results constitute the first experimental demonstration on the key role of an active transport system, that of PA, in the anaerobic catabolism of aromatic compounds.

Interestingly, the GC content of the *phtTaTb* genes from *Aromatoleum/Azoarcus/Thauera* strains (about 60% GC) is significantly lower than that of the *pht* catabolic genes (about 65% GC) which fits with the average GC content of the complete genome. Moreover, in some *pht* clusters, such as that of *A. aromaticum* EbN1, the transport genes are separated from the catabolic ones by insertion sequences (Ebenau-Jehle *et al.*, 2017). These observations suggest that *pht* transport genes may have been recruited through horizontal gene transfer during the recent ongoing evolution of *pht* clusters in bacteria that have been adapted to benefit from unusual substrates introduced by humans into the current ecosystems.

Characterization of the TAXI-TRAP transporter for PA uptake

To further confirm that the *phtTaTb* genes encode a PA transporter system and to determine its biochemical properties, we performed PA uptake experiments at different [^{14}C]-PA concentrations in *Azoarcus* sp. CIB (pIZPHT), i.e., control cells that contain only the catabolic *pht* genes, and in *Azoarcus* sp. CIB (pIZPHTRAP), i.e., cells

231 that express the catabolic *pht* genes as well as the *phtTaTb* transport genes. Whereas
232 *Azoarcus* sp. CIB (pIZPHT) cells did not show [^{14}C]-PA uptake, *Azoarcus* sp. CIB
233 (pIZPHTRAP) cells showed a maximum uptake rate of about 156 ± 14 pmol min^{-1} mg
234 protein^{-1}, with a saturation kinetics at about 20 μM PA and a transport affinity (K_m) of
235 15 μM (Fig. 4A).

236 As expected for an SBP-dependent secondary transporter, the [^{14}C]-PA uptake
237 was completely inhibited when cells were pre-incubated with DNP, but it did not
238 decrease when cells were pre-incubated with the ATP synthase inhibitor DCCD (Fig.
239 4B). These results taken together confirm that PhtTaTb constitutes a secondary
240 transporter responsible of PA uptake.

241 [^{14}C]-PA uptake rates were tested in the presence of non-radioactive phthalate
242 isomers as competitive inhibitors. As a control, when 250 μM unlabeled PA was used
243 as competitor, the uptake rate of the 25 μM [^{14}C]-PA radioactive compound was
244 undetected (Fig. 4B). Interestingly, when 250 μM unlabeled isophthalate or
245 terephthalate were used, the [^{14}C]-PA uptake rate was reduced to 50% or 60%,
246 respectively, of the rate in the absence of a competitor substrate (Fig. 4B). These
247 results suggest that although the transporter has a high affinity for PA, it shows a low
248 substrate specificity for the other two phthalate isomers.

249 The main type of SBP-dependent secondary transporters are TRAP-
250 transporters, which are usually constituted by an SBP belonging to the DctP family, and
251 by large (DctM) and small (DctQ) integral membrane proteins (Mulligan *et al.*, 2011;
252 Pietri *et al.*, 2012). TRAP-transporters involved in the transport of aromatic compounds
253 have already been characterized (Fig. 5) (Chae and Zylstra, 2006; Salmon *et al.*, 2013).
254 Interestingly, the SBP (PhtTb) protein of the two-component PA transporter does not

belong to the classical TRAP class but to a new class called TAXI-TRAP (Fig. 5). TAXI-TRAP transporters contain an SBP that does not show similarity to the SBP of classical TRAP transporters and is being called TAXI (TRAP associated extracytoplasmatic immunogenic) protein. Moreover, TAXI-TRAP transporters usually have the DctQ and DctM membrane subunits of standard TRAP transporters fused into a single integral membrane protein (Mulligan *et al*., 2011; Rosa *et al.*, 2018). Accordingly, the PhtTa protein (657 aa) of the PA transporter contains 15 predicted transmembrane segments (TM) in its structure, which are organized as 10 TM at the N-terminus (corresponding to a DctM-like large subunit), 4 TM at the C-terminus (corresponding to a DctQ-like small subunit), and an additional TM fusion segment (Supporting Information Figure S1). The only structure available for a TAXI protein, that of TT1099 from the bacterium *Thermus thermophilus* (Takahashi *et al*., 2004), reinforced its predicted role as putative glutamate transporter (Rabus *et al.*, 1999). Examination of the genome context of TAXI genes in archaea also suggests that they may be involved in transport of glutamate/glutamine or closely related C5-dicarboxylates such as 2-oxoglutarate (Mulligan *et al.*, 2011; Rosa *et al*., 2018). However, to our knowledge, the PhtTaTb transporter described in this work represents the first TAXI-TRAP transporter whose biological function has been characterized.

It is worth noting that *phtTaTb* orthologs can be also identified in clusters involved in phthalate degradation via classical aerobic pathways (Fig. 5). Thus, the *opa* cluster for PA degradation via 2,3-dihydroxybenzoate in *Pseudomonas* sp. strain PTH10 encodes the *opaL* and *opaN* gene products (Kasai *et al.*, 2019) that show 28% and 42 % identity to the *phtTb* and *phtTa* gene products, respectively. Moreover, the genomes of certain strains of *Halomonas* and *Marinobacterium* species (γ-proteobacteria), and

279 *Tistlia*, *Zhengella* and a Rhodospirillaceae bacterium (α-proteobacteria), contain *phtTb*
280 orthologs (Fig. 5) within clusters that are likely responsible for aerobic PA degradation
281 via the classical protocatechuate pathway. Therefore, the predicted role of TAXI-TRAP
282 systems for the uptake of PA in bacteria belonging to different phylogenetic groups
283 provides further insights into the functionality of this poorly characterized class of
284 secondary SBP-dependent transporters. Moreover, this work extends the current view
285 on the diversity of transport systems for the uptake of phthalates by bacteria, which
286 spans from mono-component inner membrane MFS transporters, e.g. OphD and MopB
287 (Saint and Romas, 1996; Chang *et al*., 2009), to multi-component SBP-dependent
288 transporters of all major families, i.e., primary ABC-type (e.g., OphFGH, PatDABC)
289 (Chang *et al.*, 2009), and secondary TTT-type (TpiABTphC for terephthalate, TpiABIphC
290 for isophthalate) (Fukuhara *et al.*, 2010; Hosaka *et al.*, 2013), and TRAP-type (PhtTaTb)
291 (this work) (Fig. 5).
292
293 *The peripheral pht pathway allows aerobic degradation of PA in denitrifying bacteria*
294 The pht pathway was reported to be an anaerobic peripheral pathway (Ebenau-Jehle
295 *et al*., 2017; Mergelsberg *et al*., 2017; Boll *et al.*, 2020). However, we unexpectedly
296 observed that *Azoarcus* sp. CIB (pIZPHTRAP) expressing the complete *pht* cassette was
297 also able to grow under aerobic conditions when using PA as sole carbon and energy
298 source (Fig. 3C). These PA-grown cells showed a significant induction of the
299 endogenous *boxB* gene encoding a key enzyme of the aerobic hybrid pathway for
300 benzoyl-CoA degradation (Supporting Information Figure S2) (Valderrama *et al*., 2012).
301 Therefore, these results strongly suggest that the pht pathway could allow the aerobic

302 metabolism of PA via benzoyl-CoA when the cells are equipped with an aerobic box
303 pathway.

304 To further confirm this assumption and to discard that an enzyme from the CIB
305 strain expressed in aerobically-grown *Azoarcus* sp. CIB (pIZPHTRAP) cells could
306 functionally replace the PCD decarboxylase activity (which was shown to be oxygen
307 sensitive in *in vitro* assays (Ebenau-Jehle *et al.*, 2017; Mergelsberg *et al.,* 2017)), we
308 constructed a mutant *pht* cassette without an active *phtDa* gene. When the resulting
309 plasmid pIZPHTRAP∆*phtDa* was transferred to *Azoarcus* sp. CIB, the recombinant strain
310 failed to grow on PA either in the presence or absence of oxygen (Figs. 3B and 3C),
311 strongly suggesting that *phtDa* is essential and that no other enzyme encoded in the
312 genome of the CIB strain can replace this function. In agreement with these findings,
313 we have additionally confirmed that *A. evansii*, which is also equipped with a box
314 pathway (Gescher *et al.*, 2005), was also able to use PA as sole carbon and energy
315 source in the presence of oxygen (Supporting Information Figure S3).

316 Classical aerobic PA pathways rely on ring-hydroxylating dioxygenases which
317 require oxygen tensions that may quickly become limiting in many natural ecosystems
318 or when bacteria grow on surfaces forming biofilms (Boll *et al*., 2020). The results
319 presented here unravel a new function for the pht peripheral pathway as an
320 alternative route for aerobic PA degradation in denitrifying bacteria that thrive in
321 environments that face oxygen limitations or fluctuating oxygen tensions.

322

323 *Aerobic degradation of PA via the pht pathway requires a functional box central*
324 *pathway*

When *Azoarcus* sp. CIB grows on the presence of oxygen, benzoyl-CoA can only be degraded through the hybrid box pathway (Valderrama *et al*., 2012). However, conversion of benzoyl-CoA to free benzoate by the action of specific or unspecific thioesterase and/or CoA-transferase activities (Ismail, 2008) could be proposed also as an alternative mechanism for aerobic benzoyl-CoA degradation in bacteria that harbour a classical aerobic ben (oxidizes benzoate to catechol)-cat (converts catechol to central metabolism) pathway (Fig. 6A) (Dagley *et al*., 1960; Stanier and Ornston, 1973; Harwood and Parales, 1996; Pérez-Pantoja *et al*., 2008; Díaz *et al.*, 2013; Nogales *et al.*, 2017).

To explore which should be the catabolic requirements of a bacterial host to allow aerobic mineralization of PA via the pht peripheral pathway, we transferred plasmid pIZPHTRAP to different bacterial species unable to degrade PA and that contain different combinations of hybrid (*box*) and/or classical (*ben-cat)* benzoate-degradation clusters. Thus, we generated recombinant strains of *P. putida* KT2440, which contains only the *ben-cat* genes (Jiménez *et al*., 2002), *Cupriavidus pinatubonensis* JMP134, which contains a set of *ben-cat* genes and a set of *box* genes (Pérez-Pantoja *et al*., 2008), and *C. necator* H16 (formerly known as *Ralstonia eutropha* H16), which contains a set of *ben-cat* genes in chromosome 1, a *box* cluster in chromosome 1 (box_1), and a second *box* cluster in chromosome 2 (box_2) (Pohlmann *et al.*, 2006) (Table 1).

Whereas *P. putida* KT2440 (pIZPHTRAP) and *C. pinatubonensis* JMP134 (pIZPHTRAP) grew on benzoate, they did not grow on PA. However, *C. necator* H16 (pIZPHTRAP) was able to consume PA and grow aerobically on this aromatic compound as sole carbon source (Fig. 6B). These results suggested that the classical ben-cat

pathway was not able to metabolize the benzoyl-CoA generated by the peripheral pht pathway (in agreement with the observation that a putative benzoyl-CoA thioesterase encoding gene is lacking in the genome of these strains), and that only cells expressing a functional box pathway could allow aerobic mineralization of PA via benzoyl-CoA (Fig. 6A). In this sense, it should be mentioned that although strain JMP134 contains a *box* cluster in its genome, this cluster might not encode a functional box pathway since it lacks the *boxD* gene (Gescher *et al*., 2006; Pérez-Pantoja *et al.*, 2008) and does not allow growth on benzoate to a JMP134Δ*benA* mutant strain (Donoso *et al.*, 2011; Pérez-Pantoja *et al.*, 2015).

To confirm that *C. necator* H16 (pIZPHTRAP) was degrading PA via the box pathway, we analyzed the expression of some marker genes of the classical ben-cat pathway, e.g. *benA* gene, and the hybrid box pathway, e.g., $boxB_1$ (for cluster box_1) and $boxB_2$ (for cluster box_2) (Fig. 6C). Real time RT-PCR gene expression studies of *C. necator* H16 (pIZPHTRAP) cells grown aerobically on PA were compared with those of cells grown on pyruvate (control). Whereas the basal expression of the *benA* gene was similar in pyruvate and PA, the $boxB_1$ and $boxB_2$ genes were induced in PA around 40- and 400-fold, respectively. These results suggest that *C. necator* H16 (pIZPHTRAP) cells grown on PA cannot generate free benzoate which has been shown to be the inducer of the *ben* genes in *Cupriavidus* strains (Donoso *et al.*, 2011; Pérez-Pantoja *et al.*, 2015). On the contrary, the results presented strongly suggest that an efficient metabolic flux for PA degradation via the pht pathway requires the coupling to a hybrid box pathway rather than to a classical ben-cat pathway.

Whereas the classical ben-cat benzoate degradation pathway has been extensively studied in a wide variety of bacteria, the aerobic hybrid box pathway has

been characterized more recently (Fuchs *et al*., 2011). Although *in silico* studies suggest that *box* genes are spread among α-, β- and some δ-proteobacteria (Valderrama *et al*., 2012; Suvorova and Gelfand, 2019), there are only few reports demonstrating an active box pathway in certain strains and none of them belong to the *Cupriavidus* genus (Gescher *et al.*, 2005; Gescher *et al.*, 2006; Denef *et al*., 2006; Bains *et al*., 2009; Valderrama *et al.*, 2012; Chen *et al*., 2014). Therefore, the results presented here with *Cupriavidus* strains reveal that the *pht* cassette becomes a useful genetic tool to screen for functional box pathways in bacteria by monitoring growth on PA.

Moreover, this work provides additional clues to the physiological role of *box* genes present in aerobic microorganisms endowed with classical benzoate degradation pathways (*ben-cat* genes). It was generally thought that in these microorganisms the box pathway allows growth on benzoate under reduced oxygen tensions (transition to stationary phase) or when the main ben pathway is mutated (Denef *et al.*, 2005; Denef *et al*., 2006). We propose that the box pathway is also an adaptive trait of ecological value when cells acquire metabolic modules that lead to the formation of benzoyl-CoA. We have shown this here with the *pht* cassette as a proof of concept, but the natural location of *pht* genes either in plasmids or in chromosomal regions flanked by transposases and inverted repeats (Ebenau-Jehle *et al.*, 2017; Boll *et al.*, 2020), might also facilitate their horizontal transfer and the spread of the PA degradation capability among recipient bacteria that harbour a functional box pathway.

The pht *cassette as a biotechnological tool to valorize PA*

As indicated above, PA is emerging as a feedstock generated in high amounts from the plastics additives. Phthalates account for about 60 % of the world consumption of plasticizers that is predicted to be of 12.1 M tons by 2024 (Wei and Zimmermann, 2917; Brandon and Criddle, 2019; Boll *et al*., 2020). Therefore, the use of PA as feedstock for the microbial synthesis of value added biodegradable polymers, such as polyhydroxyalkanoates (PHAs), could be a promising approach in the up-coming plastic recycling industrial processes (Prieto, 2016; Wackett, 2019; *A European Strategy for Plastics in a Circular Economy*, https://ec.europa.eu/environment/waste/plastic_waste.htm). PHAs are an environmentally friendly alternative to chemically synthesized plastics due to the fact that they are bio-based, biodegradable, biocompatible, and their material properties are similar to those of petroleum-based plastics (Prieto, 2016; Mozejko-Ciesielska and Kiewisz, 2016; Chen and Jiang, 2018). A common type of PHAs is polyhydroxybutyrate (PHB), which contains only the 3-hydroxybutyrate monomer in its composition (Rehm, 2003). Here we aimed to show the use of the recombinant *pht* cassette as a biotechnological tool for the bioconversion of PA to PHB.

C. necator H16 is an industrially relevant microorganism generally used for its high production of PHB that can account up to 80% of the total cell dry weight (Anderson and Dawes, 1990; Linko *et al*., 1993). PHB production from acetyl-CoA involves the *phaAB* and *phaC* gene products (Fig. 7A) (Pohlmann *et al.*, 2006; Brigham *et al*., 2012). Although the H16 strain has been shown to accumulate PHB granules when grown on a wide range of substrates, including certain aromatic compounds such as 4-hydroxybenzoate, 3-hydroxybenzoate, protocatechuate, gentisate,

(Tomizawa *et al*., 2014; Kumar *et al.*, 2019), the strain has never been tested for bioconversion of phthalates. Since we have shown above that the pht pathway is functional in strain H16, we tested whether *C. necator* H16 (pIZPHTRAP) cells grown aerobically on PA were able to accumulate PHB. Interestingly, PHB granules were observed inside the recombinant H16 cells (Fig. 7B). PHB monomer composition and cellular PHB content of lyophilized cells were determined by gas chromatography-tandem mass spectrometry (GC-MS) of the methanolysed polyester. Cells were able to accumulate PHB that accounted for 8-10% of the total cell dry weight. A similar percentage of PHB (14%) was accumulated when *C. necator* H16 (pIZPHTRAP) cells were grown on benzoate as sole carbon source. The composition of PHB was determined by GC-MS, and a single peak corresponding to the 3-hydroxybutyrate monomer was observed (Supporting Information Figure S4). Thus, all these results taken together reveal that *C. necator* H16 (pIZPHTRAP) strain constitutes a biotechnologically relevant biocatalyst to valorize PA towards the synthesis of PHB. Moreover, our work highlights that the aerobic hybrid box pathway becomes a suitable alternative to the classical aerobic degradation pathways (ben-cat pathways) for channelling benzoate and benzoate-generating aromatic compounds to the production of PHAs (Fig. 7A).

On the other hand, we checked whether the oxygen-independent *pht* cassette allowed also PA valorization to PHB under anaerobic conditions. Since *Azoarcus* sp. CIB has been shown to accumulate PHB when degrading aromatic hydrocarbons through the anaerobic benzoyl-CoA pathway (*bzd-pim-gcd* genes) (Zamarro *et al*., 2017), we used this strain as host for testing anaerobic valorization of PA. *Azoarcus* sp. CIB (pIZPHTRAP) strain growing anaerobically on PA was shown to produce PHB, although

445 with a 5-fold lower efficiency than that of the recombinant *C. necator* H16 strain,
446 suggesting that these cells were able to re-route part of the 3-hydroxybutyryl-CoA
447 generated in the anaerobic benzoyl-CoA pathway as substrate of the PhaC synthase
448 that generates PHB (Fig. 7A).
449
450 **Conclusions**
451 We have demonstrated that PA degradation in denitrifying bacteria via the pht
452 peripheral pathway requires an SBP-dependent secondary transporter (PhtTaTb) for
453 the uptake of PA inside the bacterial cell. The presence of *phtTaTb* genes associated to
454 putative PA degradation clusters in bacteria belonging to different phylogenetic groups
455 reinforces the physiologial role and ecological significance for bioremediation of this
456 transporter that belongs to the poorly characterized class of TAXI-TRAP transporters.
457 The pht pathway has been successfully transferred to heterologous hosts unable to
458 degrade PA. Despite pht was initially characterized as an anaerobic pathway for the
459 conversion of PA to benzoyl-CoA (Boll *et al.*, 2020), our results expand its function as
460 an alternative peripheral route for the aerobic degradation of PA when coupled to a
461 functional box central pathway. It is worth mentioning that during the evaluation of
462 this work a similar conclusion has been achieved by Ebenau-Jehle *et al.* (2020) using a
463 biochemical approach, thus reinforcing our results. Hence, the pht pathway may
464 constitute an evolutionary acquisition for PA degradation by bacteria that thrive either
465 in anoxic environments, or in environments that face oxygen limitations and that rely
466 on benzoyl-CoA, rather than on catecholic central intermediates, for the aerobic
467 catabolism of aromatic compounds. The aerobic and anaerobic valorization of PA
468 towards the biosynthesis of bioplastics, e.g., PHB, in suitable recombinant biocatalysts

469 expressing a *pht* cassette was demonstrated as a proof of concept. Nevertheless,
470 further optimization of the bioconversion efficiencies is needed for industrial
471 applications.
472
473 **Experimental Procedures**
474 *Bacterial strains, plasmids and growth conditions*
475 The bacterial strains and plasmids used are listed in Table 1. *Escherichia coli* and
476 *Pseudomonas putida* cells were grown at 37 °C or 30 °C, respectively, on lysogeny
477 broth (LB) medium (Miller, 1972). *Azoarcus* and *Aromatoleum* strains were grown
478 anaerobically at 30 °C on MC minimal medium (López-Barragán *et al*., 2004) using the
479 indicated carbon source(s) and 10 mM nitrate as the terminal electron acceptor.
480 *Azoarcus, Aromatoleum* and *Cupriavidus* strains were grown aerobically at 30 °C on NB
481 medium (Difco, 234000) or on MC minimal medium supplemented with the indicated
482 carbon source(s) but without nitrate. When needed, gentamicin (7.5 μg/ml) and 1 mM
483 isopropyl β-D-1-thiogalactopyranoside (IPTG) (to induce heterologous *pht* expression)
484 were added.
485 *Molecular biology techniques*
486 Standard molecular biology techniques were performed as previously described
487 (Sambrook and Russell, 2001). Plasmid DNA was prepared with a High Pure plasmid
488 isolation kit (Roche Applied Science). DNA fragments were purified with Gene-Clean
489 Turbo (Q-BIOgene). Gibson Assembly was performed following the published methods
490 (Gibson *et al.*, 2009). All cloned inserts and DNA fragments were confirmed by DNA
491 sequencing through an ABI Prism 377 automated DNA sequencer (Applied Biosystems

Inc.). Oligonucleotides employed are listed in Supporting Information Table S1. Transformation of *E. coli* cells was carried out by using the RbCl method or by electroporation (Gene Pulser; Bio-Rad) (Sambrook and Russell, 2001). Plasmids were transferred from *E. coli* S17–1λpir (donor strain) into *Azoarcus, Cupriavidus* and *P. putida* recipient strains by biparental filter mating as described previously (López-Barragán *et al.*, 2004). The protein concentration in cell extracts was determined by the method of Bradford (Bradford, 1976) by using bovine serum albumin as the standard.

Construction of the pht *cassette and derivatives*

The pIZPHT plasmid was constructed by amplifying the region 66351-71015 bp of plasmid 2 from *A. aromaticum* EbN1 with the EbN1 113 FW/ EbN1 102 RV primers (Supporting Information Table S1). The DNA fragment was further digested with *Hin*dIII/*Spe*I and ligated to the pIZ1016 vector (*Hin*dIII/*Spe*I digested) by T4 ligase treatment. The pIZPHTRAP plasmid was constructed by amplifying the region 61.439-65.196 bp of plasmid 2 from *A. aromaticum* EbN1 with the 97 FW Gibson/ 95 Rv Gibson primers (Supporting Information Table S1). The DNA fragment was introduced into pIZPHT (*Spe*I digested) by Gibson Assembly protocol (Gibson *et al.*, 2009). The pIZPHTRAPΔphtDa plasmid was constructed from *Sna*BI/*Sph*I double- digested pIZPHTRAP plasmid (which releases a 591-bp internal fragment of *phtDa* gene) which was blunt-ended with Klenow enzyme and then circularized after T4 ligase treatment.

Sequence data analyses

A homology search of *phtTaTb*-like genes in finished and unfinished microbial genome databases was performed with the TBLASTN algorithm (Altschul *et al*., 1990) at the NCBI server (https://blast.ncbi.nlm.nih.gov/Blast.cgi). Multiple sequence alignment of amino acid sequences from solute binding-protein (SBP) of different primary (ABC-type) and secondary (TRAP-, TTT-, TAXI-TRAP-type) transporters was performed using Clustal Omega alignment tool with default parameters (https://www.ebi.ac.uk/Tools/msa/clustalo/). Phylogenetic analysis was performed using the neighbour-joining statistical method based on the Poisson correction model, and a tree was reconstructed using the neighbour-joining method at the EBI server (https://www.ebi.ac.uk/Tools/msa/clustalo/). The prediction of transmembrane segments in the PhtTa protein was performed by using the TMHMM 2.0 program at the DTU Health Tech server from Technical University of Denmark (http://www.cbs.dtu.dk/services/TMHMM/).

PA uptake assays

A. evansii cells were grown on MC medium with 3 mM benzoate or 3 mM PA as sole carbon source for 24 h. *Azoarcus* sp. CIB cells containing plasmids pIZPHT or pIZPHTRAP (Table 1) were grown on NB medium with 1.0 mM IPTG, to induce the expression of the cloned *pht* genes, for 16 h until reaching the stationary phase (A_{600} of 1.8). Cells were harvested by centrifugation, washed twice and suspended into saline solution to an A_{600} of 4.0. The standard PA uptake assay contained 50 μL of cells pre-warmed at 30 °C for 5 min, and 5 μL of 250 μM [carboxyl-^{14}C]-PA (50 μCi/mmol ARC 1057; American Radiolabeled Chemicals). Samples were incubated with shaking for 5 min at 30°C, and the assay was stopped by adding 1 mL of ice-cold saline solution and

by filtrating the cells through a 0.22 μm pore-size GSWP nitrocellulose filter (Millipore). Concentrated cells were washed with 5 mL of ice-cold saline solution, the [^{14}C]-PA accumulated inside the cells was determined by scintillation counting in an LKB Wallac liquid scintillation counter as previously described (Prieto and García, 1997). Where indicated, different amounts of [^{14}C]-PA or incubation times were used. Uptake rates were calculated relative to the amount of cells (biomass was determined by total protein in crude cell extracts) used in the transport assays.

RNA extraction and RT-PCR assays

C. necator H16 and *Azoarcus* sp. CIB cells harbouring plasmid pIZPHTRAP were grown aerobically on PA-, benzoate- or pyruvate-containing MC medium until the culture reached the end of the exponential phase. Cells were centrifuged, lysed for 10 min at 37 ºC in TE buffer (10 mM Tris-HCl, pH 7.5, 1 mM EDTA) containing 50 mg ml^{-1} lysozyme. Total RNA was extracted using a High Pure RNA isolation kit (Roche), and DNase-treated with a Turbo DNase kit (Ambion). The concentration and purity of the RNA samples were assessed using the Nanophotometer Pearl (Implen), according to the manufacturer's protocol, and by testing the absence of DNA (*recA* gene) through PCR amplification.

The synthesis of total cDNA was performed by using the Transcriptor First Strand cDNA Synthesis kit (Roche) in 20-μl reactions containing 1 μg of RNA, 1 mM concentration of each dNTP, 10 units of reverse transcriptase, 20 units of Protector RNase Inhibitor, and 60 μM random hexamers as primers in the buffer provided by the manufacturer. The RNA and hexamers were initially heated at 65 °C for 10 min and following the addition of the rest of the components, samples were incubated at 25°C

for 10 min and then at 55°C for 30 min. Reactions were terminated by incubation at 85°C for 5 min. In standard RT-PCR reactions, the cDNA was amplified with 1 unit of AmpliTaq DNA polymerase (Biotools) and 0.5 μM concentrations of the corresponding primer pairs of the *boxB* gene from *Azoarcus* sp. CIB (Supporting Information Table S1). Control reactions in which reverse transcriptase was omitted from the reaction mixture ensured that DNA products resulted from the amplification of cDNA rather than from DNA contamination. Real-time PCR assays were performed as described previously (Martín-Moldes *et al.*, 2016), in a LightCycler®480 II real-time PCR system (Roche). The analysis was performed in three technical replicates from three biological samples. Reactions (20 μl) contained 1 μl (2.5 ng) of cDNA, 0.25 μM of each of the two target-specific primers, and 10 μl of SYBR Green I Master Mix (Roche). Oligonucleotides used to amplify transcripts from the *benA*, $boxB_1$, $boxB_2$ and the *recA* gene of strain H16, the last one used as housekeeping (internal standard), are listed in Supporting Information Table S1. PCR amplifications were carried out with one denaturation cycle (95 °C for 5 min), followed by 30 cycles of amplification (95 °C for 10 s, 60 °C for 10 s, and 72 °C for 10 s). After amplification, 7 melting curves were generated to confirm amplification of a single product. For relative quantification of the fluorescence values, a calibration curve was constructed by sevenfold serial dilutions of a *C. necator* H16 genomic DNA sample ranging from 1 ng to 0.5 $x10^{-7}$ ng. This curve was then used as a reference standard for extrapolating the relative abundance of the cDNA target within the linear range of the curve.

Transmission electron microscopy (TEM) studies

586 Bacterial cells were harvested, washed twice in saline solution and fixed in 5% (w/v)
587 glutaraldehyde. Afterwards, cells were suspended in 2.5% (w/v) OsO_4 for 1 h, gradually
588 dehydrated in ethanol solutions [30%, 50%, 70%, 90% and 100% (v/v); 30 min each)
589 and propylene oxide (1h), and embedded in Epon 812 resin. Ultrathin sections were
590 cut with a microtome using a Diatome diamond knife. The sections were picked up
591 with 400 mesh cupper grids coated with a layer of carbon, and observed using a Jeol-
592 1230 transmission electron microscope.
593
594 *Analysis of PHB content and monomer composition*
595 To determine the PHB content of *Azoarcus* sp. CIB and *C. necator* H16 strains
596 harbouring plasmid pIZPHTRAP, cells were grown at 30 °C on MC medium with 3 mM
597 benzoate or 3 mM PA under anaerobic or aerobic conditions, respectively, until they
598 reached the stationary phase. PHB production was quantified by GC-MS of the
599 methanolysed polyester and shown as the percentage of PHB monomer with respect
600 to the total cell dry weight (CDW). Methanolysis procedure was carried out by
601 suspending 5-10 mg of lyophilized cells in 2 ml of methanol containing 3% sulfuric acid
602 and 2 ml of a solution of 0.5 mg ml^{-1} of 3-methylbenzoic acid (internal standard) in
603 chloroform, and then incubated at 100 °C for 5 h in a sealed tube under stirring. After
604 cooling, 1 ml of de-mineralized water was added, the mixture was vigorously stirred,
605 and two phases were obtained (this step was repeated twice). The organic phase
606 containing the resulting methyl esters of monomers was analyzed by GC-MS (de
607 Eugenio *et al.*, 2010). An Agilent series 7890A gas chromatograph coupled with 5975C
608 MS detector (EI, 70 eV) and a split/splitless injector were used for analysis. An aliquot
609 (1 μl) of the organic phase was injected into the gas chromatograph at a split ratio

1:20. Separation of compounds was achieved using a DB-5ht (-60 ºC-400 °C: 30 m *0.25 mm * 0.1 μm film thickness) column. Helium was used as carrier gas at a flow rate of 1 ml min^{-1}. The injector and transfer line temperature were set at 275 °C and 280 °C, respectively. The oven temperature program was initial temperature 60 °C for 2 min, then from 60 °C up to 65 °C at a rate of 5 °C/min, and then from 65 °C up to 125 °C at a rate of 10 °C/min. EI mass spectra were recorded in full scan mode (m/z 40–550).

Consumption of PA in bacterial cultures

The presence of residual PA was quantified by HPLC (Agilent Series 1260 Infinity II, Agilent, CA, USA) using a Mediterranea™ sea18 (TEKNOKROMA) (15 cm x 0,46 cm, 5 μm particle size) column, at room temperature with a flow rate of 1 mL min^{-1} and an injection volume of 25 μl. The mobile phase was 0.1 % trifluoroacetic acid both in water (A) and acetonitrile (B). The elution program was used as follows: at the start, 100 % A; after 5 min, the percentage of B was linearly increased to 100 % in 20 min. After that, it was ramped to the original composition (100% A) in 2 min, and then equilibrated for 5 min. The retention time of PA was 13.1 min. A standard curve of PA was done (1-5 mM). To demonstrate that the medium does not contain any interfering substance in the chromatogram, the medium without PA was injected as control.

Acknowledgments

We thank A. Valencia for technical assistance. We acknowledge J. García, and N. Hernández, V. Rivero-Buceta and A. Prieto for their advices in transport assays and PHB analyses, respectively. Support was provided by grants BIO2016-79736-R and PCIN-2014-113 from the Ministry of Economy and Competitiveness of Spain; by a grant from the Fundación Ramón-Areces XVII CN; by Grant CSIC 2016 2 0E 093; and by European Union H2020 Grant 760994. D. Sanz was the recipient of a FPU14/04356 fellowship from the Ministry of Education, Culture and Sports.

Conflict of interest

The authors declare that there is no conflict of interest.

References

Altschul, S.F., Gish, W., Miller, W., Myers, E.W., and Lipman, D.J. (1990) Basic local alignment search tool. *J Mol Biol* **215:** 403–410.

Anders, H.J., Kaetzke, A., Kämpfer, P., Ludwig, W., and Fuchs, G. (1995) Taxonomic position of aromatic-degrading denitrifying pseudomonad strains K 172 and KB 740 and their description as new members of the genera *Thauera*, as *Thauera aromatica* sp. nov., and *Azoarcus*, as *Azoarcus evansii* sp. nov., respectively, members of the beta subclass of the Proteobacteria. *Int J Syst Bacteriol* **45:** 327–333.

Anderson, A.J., and Dawes, E.A. (1990) Occurrence, metabolism, metabolic role, and industrial uses of bacterial polyhydroxyalkanoates. *Microbiol Rev* **54:** 450–472.

Annamalai, J., and Namasivayam, V. (2015) Endocrine disrupting chemicals in the atmosphere: their effects on humans and wildlife. *Environ Int* **76:** 78–97.

Bains, J., Leon, R., and Boulanger, M.J. (2009) Structural and biophysical characterization of BoxC from *Burkholderia xenovorans* LB400: a novel ring-cleaving enzyme in the crotonase superfamily. *J Biol Chem* **284:** 16377–16385.

Benjamin, S., Pradeep, S., Josh, M.S., Kumar, S., and Masai, E. (2015) A monograph on the remediation of hazardous phthalates. *J Hazard Mater* **298:** 58–72.

678 Boll, M., Geiger, R., Junghare, M., and Schink, B. (2020) Microbial degradation of
679 phthalates: biochemistry and environmental implications. *Environ Microbiol Rep* **12:**3-
680 15.
681 Bradford, M.M. (1976) A rapid and sensitive method for the quantitation of microgram
682 quantities of protein utilizing the principle of protein-dye binding*. Anal Biochem* **72:**
683 248–254.
684 Brandon, A.M., and Criddle, C.S. (2019) Can biotechnology turn the tide on plastics?
685 *Curr Opin Biotechnol* **57:** 160–166.
686
687 Brigham, C.J., Zhila, N., Shishatskaya, E., Volova, T.G., and Sinskey, A.J. (2012)
688 Manipulation of *Ralstonia eutropha* carbon storage pathways to produce useful bio-
689 based products. In *Reprogramming Microbial Metabolic Pathways*. Wang *et al.* (eds).
690 Dordrecht: Springer, pp. 343-366.
691 Carmona, M., Zamarro, M.T., Blázquez, B., Durante-Rodríguez, G., Juárez, J.F.,
692 Valderrama, J.A., *et al*. (2009) Anaerobic catabolism of aromatic compounds: a genetic
693 and genomic view. *Microbiol Mol Biol Rev* **73:** 71–133.
694 Chae, J.-C., and Zylstra, G.J. (2006) 4-Chlorobenzoate uptake in *Comamonas* sp. strain
695 DJ-12 is mediated by a tripartite ATP-independent periplasmic transporter. *J Bacteriol*
696 **188:** 8407–8412.
697 Chang, H.-K., Dennis, J.J., and Zylstra, G.J. (2009) Involvement of two transport systems
698 and a specific porin in the uptake of phthalate by *Burkholderia* spp. *J Bacteriol* **191:**
699 4671–4673.

Chen, D.-W., Zhang, Y., Jiang, C.-Y., and Liu, S.-J. (2014) Benzoate metabolism intermediate benzoyl coenzyme A affects gentisate pathway regulation in *Comamonas testosteroni*. *Appl Environ Microbiol* **80:** 4051–4062.

Chen, G.-Q., and Jiang, X.-R. (2018) Engineering microorganisms for improving polyhydroxyalkanoate biosynthesis. *Curr Opin Biotechnol* **53:** 20–25.

Dagley, S., Evans, W.C., and Ribbons, D. W. (1960) New pathways in the oxidative metabolism of aromatic compounds by micro-organisms. *Nature* **188:** 560-566.

de Eugenio, L.I., Escapa, I.F., Morales, V., Dinjaski, N., Galán, B., García, J.L., *et al*. (2010) The turnover of medium-chain-length polyhydroxyalkanoates in *Pseudomonas putida* KT2442 and the fundamental role of PhaZ depolymerase for the metabolic balance. *Environ Microbiol* **12:** 207–221.

de Lorenzo, V., and Timmis, K.N. (1994) Analysis and construction of stable phenotypes in gram-negative bacteria with Tn5- and Tn10-derived minitransposons. *Methods Enzymol* **235:** 386–405.

Denef, V.J., Klappenbach, J.A., Patrauchan, M.A., Florizone, C., Rodrigues, J.L., Tsoi, T.V., *et al*. (2006) Genetic and genomic insights into the role of benzoate-catabolic pathway redundancy in *Burkholderia xenovorans* LB400. *Appl Environ Microbiol* **72:** 585–595.

Denef, V.J., Patrauchan, M.A., Florizone, C., Park, J., Tsoi, T.V., Verstraete, W., *et al*. (2005) Growth substrate- and phase-specific expression of biphenyl, benzoate, and C1 metabolic pathways in *Burkholderia xenovorans* LB400. *J Bacteriol* **187:** 7996–8005.

Díaz, E., Jiménez, J.I., and Nogales, J. (2013) Aerobic degradation of aromatic compounds. *Curr Opin Biotechnol* **24:** 431–442.

723 Don, R.H., and Pemberton, J.M. (1981) Properties of six pesticide degradation plasmids
724 isolated from *Alcaligenes paradoxus* and *Alcaligenes eutrophus*. *J Bacteriol* **145:** 681–
725 686.

726 Donoso, R.A., Pérez-Pantoja, D., and González, B. (2011) Strict and direct
727 transcriptional repression of the *pobA* gene by benzoate avoids 4-hydroxybenzoate
728 degradation in the pollutant degrader bacterium *Cupriavidus necator* JMP134. *Environ*
729 *Microbiol* **13:** 1590–1600.

730 Eaton, R.W., and Ribbons, D.W. (1982) Metabolism of dibutylphthalate and phthalate
731 by *Micrococcus* sp. strain 12B. *J Bacteriol* **151:** 48–57.

732 Ebenau-Jehle, C., Mergelsberg, M., Fischer, S., Brüls, T., Jehmlich, N., von Bergen, M.,
733 *et al*. (2017) An unusual strategy for the anoxic biodegradation of phthalate. *ISME J* **11:**
734 224–236.

735 Ebenau-Jehle, C., Soon, C.I.S.L., Fuchs, J., Geiger, R., and Boll, M. (2020) An aerobic
736 hybrid phthalate degradation pathway via phthaloyl-coenzyme A in denitrifying
737 bacteria. *Appl Environ Microbiol* doi: 10.1128/AEM.00498-20.

738 Egland, P.G., Pelletier, D.A., Dispensa, M., Gibson, J., and Harwood, C.S. (1997) A
739 cluster of bacterial genes for anaerobic benzene ring biodegradation. *Proc Natl Acad*
740 *Sci USA* **94:** 6484–6489.

741 Franklin, F.C., Bagdasarian, M., Bagdasarian, M.M., and Timmis, K.N. (1981) Molecular
742 and functional analysis of the TOL plasmid pWWO from *Pseudomonas putida* and
743 cloning of genes for the entire regulated aromatic ring meta cleavage pathway. *Proc*
744 *Natl Acad Sci USA* **78:** 7458–7462.

745 Fuchs, G. (2008) Anaerobic metabolism of aromatic compounds. *Ann N Y Acad Sci*
746 **1125:** 82–99.

747 Fuchs, G., Boll, M., and Heider, J. (2011) Microbial degradation of aromatic compounds
748 -from one strategy to four*. Nat Rev Microbiol* **9:**803–816.

749 Fukuhara, Y., Inakazu, K., Kodama, N., Kamimura, N., Kasai, D., Katayama, Y., *et al*.
750 (2010) Characterization of the isophthalate degradation genes of *Comamonas* sp.
751 strain E6. *Appl Environ Microbiol* **76:** 519–527.

752 Gao, D.-W., and Wen, Z.-D. (2016) Phthalate esters in the environment: a critical
753 review of their occurrence, biodegradation, and removal during wastewater treatment
754 processes. *Sci Total Environ* **541:** 986–1001.

755 Geiger, R.A., Junghare, M., Mergelsberg, M., Ebenau-Jehle, C., Jesenofsky, V.J.,
756 Jehmlich, N., *et al*. (2019) Enzymes involved in phthalate degradation in sulphate-
757 reducing bacteria. *Environ Microbiol* **21:** 3601-3612.

758 Gescher, J., Eisenreich, W., Wörth, J., Bacher, A., and Fuchs, G. (2005) Aerobic benzoyl-
759 CoA catabolic pathway in *Azoarcus evansii*: studies on the non-oxygenolytic ring
760 cleavage enzyme. *Mol Microbiol* **56:** 1586–1600.

761 Gescher, J., Ismail, W., Olgeschläger, E., Eisenreich, W., Wörth, J., and Fuchs, G. (2006)
762 Aerobic benzoyl-coenzyme A (CoA) catabolic pathway in *Azoarcus evansii*: conversion
763 of ring cleavage product by 3,4-dehydroadipyl-CoA semialdehyde dehydrogenase. *J*
764 *Bacteriol* **188:** 2919–2927.

765 Gibson, D.G., Young, L., Chuang, R.-Y., Venter, J.C., Hutchison, C.A., and Smith, H.O.
766 (2009) Enzymatic assembly of DNA molecules up to several hundred kilobases. *Nat*
767 *Methods* **6:** 343–345.
768 Hara, H., Stewart, G.R., and Mohn, W.W. (2010) Involvement of a novel ABC
769 transporter and monoalkyl phthalate ester hydrolase in phthalate ester catabolism by
770 *Rhodococcus jostii* RHA1. *Appl Environ Microbiol* **76:** 1516–1523.

771 Harwood, C.S., and Parales, R.E. (1996) The beta-ketoadipate pathway and the biology
772 of self-identity. *Annu Rev Microbiol* **50:** 553-590.

773 Hosaka, M., Kamimura, N., Toribami, S., Mori, K., Kasai, D., Fukuda, M., *et al*. (2013)
774 Novel tripartite aromatic acid transporter essential for terephthalate uptake in
775 *Comamonas* sp. strain E6. *Appl Environ Microbiol* **79:** 6148–6155.

776 Ismail, W. (2008) Benzoyl-coenzyme A thioesterase of *Azoarcus evansii*: properties and
777 function. *Arch Microbiol* **190:** 451–460.
778 Jiménez, J.I., Miñambres, B., García, J.L., and Díaz, E. (2002) Genomic analysis of the
779 aromatic catabolic pathways from *Pseudomonas putida* KT2440. *Environ Microbiol* **4:**
780 824–841.

781 Juárez, J.F., Zamarro, M.T., Eberlein, C., Boll, M., Carmona, M., and Díaz, E. (2013)
782 Characterization of the *mbd* cluster encoding the anaerobic 3-methylbenzoyl-CoA
783 central pathway. *Environ Microbiol* **15:** 148–166.

784 Junghare, M., Spiteller, D., and Schink, B. (2016) Enzymes involved in the anaerobic
785 degradation of *ortho*-phthalate by the nitrate-reducing bacterium *Azoarcus* sp. strain
786 PA01. *Environ Microbiol* **18:** 3175–3188.

787 Junghare, M., Spiteller, D., and Schink, B. (2019) Anaerobic degradation of xenobiotic
788 isophthalate by the fermenting bacterium *Syntrophorhabdus aromaticivorans*. *ISME J*
789 **13:** 1252–1268.

790 Kasai, D., Iwasaki, T., Nagai, K., Araki, N., Nishi, T., and Fukuda, M. (2019) 2,3-
791 dihydroxybenzoate *meta*-cleavage pathway is involved in *o*-phthalate utilization in
792 *Pseudomonas* sp. strain PTH10. *Sci Rep* **9:** 1253.

793 Keyser, P., Pujar, B.G., Eaton, R.W., and Ribbons, D.W. (1976) Biodegradation of
794 phthalates and their esters by bacteria. *Environ Health Perspect* **18:**159–166.
795 Kumar, P., Maharjan, A., Jun, H.-B., and Kim, B.S. (2019) Bioconversion of lignin and its
796 derivatives into polyhydroxyalkanoates: challenges and opportunities. *Biotechnol Appl*
797 *Biochem* **66:** 153–162.

798 Liang, D.-W., Zhang, T., Fang, H.H.P., and He, J. (2008) Phthalates biodegradation in the
799 environment. *Appl Microbiol Biotechnol* **80:** 183–198.

800 Linko, S., Vaheri, H., and Seppälä, J. (1993) Production of poly-β-hydroxybutyrate by
801 *Alcaligenes eutrophus* on different carbon sources. *Appl Microbiol Biotechnol* **39:** 11–
802 15.

803 López-Barragán, M.J., Carmona, M., Zamarro, M.T., Thiele, B., Boll, M., Fuchs, G. *et al*.
804 (2004) The *bzd* gene cluster, coding for anaerobic benzoate catabolism, in *Azoarcus* sp.
805 strain CIB. *J Bacteriol* **186:** 5762–5774.

806 Marshall, S.A., Payne, K.A.P., Fisher, K., White, M.D., Ní Cheallaigh, A., Balaikaite, A., *et*
807 *al*. (2019) The UbiX flavin prenyltransferase reaction mechanism resembles class I
808 terpene cyclase chemistry. *Nat Commun* **10:**2357.

809 Martín-Moldes, Z., Blázquez, B., Baraquet, C., Harwood, C.S., Zamarro, M.T., and Díaz,
810 E. (2016) Degradation of cyclic diguanosine monophosphate by a hybrid two-
811 component protein protects *Azoarcus* sp. strain CIB from toluene toxicity. *Proc Natl*
812 *Acad Sci USA* **113:** 13174–13179.
813 Martín-Moldes, Z., Zamarro, M.T., Del Cerro, C., Valencia, A., Gómez, M.J., Arcas, A., *et*
814 *al*. (2015) Whole-genome analysis of *Azoarcus* sp. strain CIB provides genetic insights
815 to its different lifestyles and predicts novel metabolic features. *Syst Appl Microbiol* **38:**
816 462–471.

817 Mergelsberg, M., Egle, V., and Boll, M. (2018) Evolution of a xenobiotic degradation
818 pathway: formation and capture of the labile phthaloyl-CoA intermediate during
819 anaerobic phthalate degradation. *Mol Microbiol* **108:** 614–626.

820 Mergelsberg, M., Willistein, M., Meyer, H., Stärk, H.-J., Bechtel, D.F., Pierik, A.J., *et al*.
821 (2017) Phthaloyl-coenzyme A decarboxylase from *Thauera chlorobenzoica*: the
822 prenylated flavin-, K+ - and Fe2+ -dependent key enzyme of anaerobic phthalate
823 degradation. *Environ Microbiol* **19:** 3734–3744.

824 Miller, J.H. (1972) *Experiments in Molecular Genetics*. Cold Spring Harbor, NY, USA:
825 Cold Spring Harbor Laboratory Press.

826 Moreno-Ruiz, E., Hernáez, M.J., Martínez-Pérez, O., and Santero, E. (2003)
827 Identification and functional characterization of *Sphingomonas macrogolitabida* strain
828 TFA genes involved in the first two steps of the tetralin catabolic pathway. *J Bacteriol*
829 **185:** 2026–2030.
830 Możejko-Ciesielska, J., and Kiewisz, R. (2016) Bacterial polyhydroxyalkanoates: still
831 fabulous? *Microbiol Res* **192:** 271–282.

832 Mulligan, C., Fischer, M., and Thomas, G.H. (2011) Tripartite ATP-independent
833 periplasmic (TRAP) transporters in bacteria and archaea. *FEMS Microbiol Rev* **35:** 68–
834 86.

835 Nogales, J., García, J.L., and Díaz, E. (2017) Degradation of aromatic compounds in
836 *Pseudomonas*: a systems biology view. In *Aerobic Utilization of Hydrocarbons, Oils and*
837 *Lipids, Handbook of Hydrocarbon and Lipid Microbiology.* Rojo, F. (ed.) Heidelberg,
838 Germany: Springer, pp. 1–49.

839 Nozawa, T., and Maruyama, Y. (1988) Anaerobic metabolism of phthalate and other
840 aromatic compounds by a denitrifying bacterium. *J Bacteriol* **170:** 5778–5784.

841 Pérez-Pantoja, D., de la Iglesia, R., Pieper, D.H., and González, B. (2008) Metabolic
842 reconstruction of aromatic compounds degradation from the genome of the amazing
843 pollutant-degrading bacterium *Cupriavidus necator* JMP134. *FEMS Microbiol Rev* **32:**
844 736–794.

845 Pérez-Pantoja, D., Leiva-Novoa, P., Donoso, R.A., Little, C., Godoy, M., Pieper, D.H., *et*
846 *a*l. (2015) Hierarchy of carbon source utilization in soil bacteria: hegemonic preference
847 for benzoate in complex aromatic compound mixtures degraded by *Cupriavidus*
848 *pinatubonensis* strain JMP134. *Appl Environ Microbiol* **81:** 3914–3924.

849 Pietri, R., Zerbs, S., Corgliano, D.M., Allaire, M., Collart, F.R., and Miller, L.M. (2012)
850 Biophysical and structural characterization of a sequence-diverse set of solute-binding
851 proteins for aromatic compounds. *J Biol Chem* **287:** 23748–23756.

852 Pohlmann, A., Fricke, W.F., Reinecke, F., Kusian, B., Liesegang, H., Cramm, R., *et al*.
853 (2006) Genome sequence of the bioplastic-producing "Knallgas" bacterium *Ralstonia*
854 *eutropha* H16. *Nat Biotechnol* **24:** 1257–1262.

855 Prieto, A. (2016) To be, or not to be biodegradable… that is the question for the
856 bio-based plastics. *Microb Biotechnol* **9:** 652–657.

857 Prieto, M.A., and García, J.L. (1997) Identification of the 4-hydroxyphenylacetate
858 transport gene of *Escherichia coli* W: construction of a highly sensitive cellular
859 biosensor. *FEBS Lett* **414:** 293-297.

860 Rabus, R., Jack, D.L., Kelly, D.J., and Saier, M.H. (1999) TRAP transporters: an ancient
861 family of extracytoplasmic solute-receptor-dependent secondary active transporters.
862 *Microbiology* **145:** 3431–3445.

863 Rabus, R., Wöhlbrand, L., Thies, D., Meyer, M., Reinhold-Hurek, B., and Kämpfer, P.
864 (2019) *Aromatoleum* gen. nov., a novel genus accommodating the phylogenetic
865 lineage including *Azoarcus evansii* and related species, and proposal of *Aromatoleum*
866 *aromaticum* sp. nov., *Aromatoleum petrolei* sp. nov., *Aromatoleum bremense* sp. nov.,
867 *Aromatoleum toluolicum* sp. nov. and *Aromatoleum diolicum* sp. nov*. Int J Syst Evol*
868 *Microbiol* **69:** 982–997.

869 Rehm, B.H.A. (2003) Polyester synthases: natural catalysts for plastics. *Biochem J* **376:**
870 15–33.

871 Ribbons, D.W., and Evans, W.C. (1960) Oxidative metabolism of phthalic acid by soil
872 pseudomonads. *Biochem J* **76:** 310–318.

873 Rosa, L.T., Bianconi, M.E., Thomas, G.H., and Kelly, D.J. (2018) Tripartite ATP-
874 independent periplasmic (TRAP) transporters and tripartite tricarboxylate transporters
875 (TTT): from uptake to pathogenicity. *Front Cell Infect Microbiol* **8:**33.
876 Saint, C.P., and Romas, P. (1996). 4-Methylphthalate catabolism in *Burkholderia*
877 (*Pseudomonas*) cepacia Pc701: a gene encoding a phthalate-specific permease forms
878 part of a novel gene cluster. *Microbiology* **142:** 2407–2418.

879 Salmon, R.C., Cliff, M.J., Rafferty, J.B., and Kelly, D.J. (2013) The CouPSTU and TarPQM
880 transporters in *Rhodopseudomonas palustris*: redundant, promiscuous uptake systems
881 for lignin-derived aromatic substrates. *PLoSOne* **8:** e59844.

882 Sambrook, J., and Russell, D.W. (2001) *Molecular Cloning: A Laboratory Manual*. Cold
883 Spring Harbor, NY, USA: Cold Spring Harbor Laboratory Press.

884 Stanier, R.Y., and Ornston, L.N. (1973) The beta-ketoadipate pathway. *Adv Microb*
885 *Physiol* **9:** 89–151.

886 Suvorova, I.A., and Gelfand, M.S. (2019) Comparative genomic analysis of the
887 regulation of aromatic metabolism in betaproteobacteria. *Front Microbiol* **10:**642.

888 Takahashi, H., Inagaki, E., Kuroishi, C., and Tahirov, T.H. (2004) Structure of the
889 *Thermus thermophilus* putative periplasmic glutamate/glutamine-binding protein. *Acta*
890 *Crystallogr D Biol Crystallogr* **60:** 1846–1854.

891 Tomizawa, S., Chuah, J.-A., Matsumoto, K., Doi, Y., and Numata, K. (2014)
892 Understanding the limitations in the biosynthesis of polyhydroxyalkanoate (PHA) from
893 lignin derivatives. *ACS Sustainable Chem Eng* **2:**1106–1113.

Trautwein, K., Wilkes, H., and Rabus, R. (2012) Proteogenomic evidence for β-oxidation of plant-derived 3-phenylpropanoids in *"Aromatoleum aromaticum"* EbN1. *Proteomics* **12:** 1402–1413.

Valderrama, J.A., Durante-Rodríguez, G., Blázquez, B., García, J.L., Carmona, M., and Díaz, E. (2012) Bacterial degradation of benzoate: cross-regulation between aerobic and anaerobic pathways. *J Biol Chem* **287:** 10494–10508.

Wackett, L.P. (2019) Bio-based and biodegradable plastics. *Microb Biotechnol* **12:** 1492–1493.

Wei, R., and Zimmermann, W. (2017) Biocatalysis as a green route for recycling the recalcitrant plastic polyethylene terephthalate. *Microb Biotechnol* **10:** 1302–1307.

Zamarro, M.T., Barragán, M.J.L., Carmona, M., García, J.L., and Díaz, E. (2017) Engineering a *bzd* cassette for the anaerobic bioconversion of aromatic compounds. *Microb Biotechnol* **10:** 1418–1425.

915

916

917

918

919

920

921

922 **Figure legends**

923

924 **Fig. 1.** Scheme of the biochemistry and associated genetic determinants of the *pht*
925 peripheral pathway for PA degradation in denitrifying bacteria.

926 A. Uptake of PA inside the bacterial cell by a putative solute-binding protein (SBP)
927 transporter (PhtTaTb) is indicated with a grey arrow. Activation of PA to *o*-phthaloyl-
928 CoA by the SPT CoA transferase (PhtSaSb) is shown with a black arrow.
929 Decarboxylation of *o*-phthaloyl-CoA to benzoyl-CoA by a PCD decarboxylase (PhtDa
930 and its associated PhtDb FMN prenyltransferase) is shown with a white arrow.
931 Benzoyl-CoA is finally de-aromatized and funnelled into the tricarboxylic acid cycle
932 (TCA) via the anaerobic bzd central pathway.

933 B. General organization of the PA-induced *pht* gene cluster. The colour code of the
934 genes corresponds to that of the functions indicated in panel A. In obligate anaerobes,

935 the *pht* gene cluster shows a similar organization but the *phtSaSb* genes are replaced
936 by a single gene encoding a PA CoA ligase.

937

938 **Fig. 2.** Uptake of PA by *A. evansii* cells grown under nitrate-reducing conditions.

939 A. The [^{14}C]-PA uptake assays were performed with cells grown on benzoate (white
940 bars) or PA (black bars). Graphed values are the average of three independent
941 experiments (error bars indicate standard deviations).

942 B. Effect of energetic inhibitors on [^{14}C]-PA uptake in *A. evansii* cells grown
943 anaerobically on PA. Cells were grown and then exposed or not (None) to 1 mM DNP
944 (proton-motive force blocking agent 2,4-dinitrophenol) or 1 mM DCCD (ATP synthase
945 inhibitor dicyclohexylcarbodiimide) before performing the [^{14}C]-PA uptake assays.
946 Graphed values are the average of three independent experiments (error bars indicate
947 standard deviations).

948

949 **Fig. 3.** Expression of the *pht* cassette in *Azoarcus* sp. CIB cells.

950 A. Scheme of the *pht* cassette cloned into the broad-host range pIZPHTRAP plasmid.
951 The *pht* genes are indicated by white, black and grey thick arrows. Some restriction
952 sites are indicated: M, *Mfe*I, S, *Sgr*DI, Sp, *Spe*I, X, *Xba*I. The gentamicin resistance gene
953 (Gm^r), mobilization (*mob*), broad-host range origin of replication (bhr *ori*), and the
954 regulatory couple *lacI*^{q} repressor gene (*lacI*^{q}) and *Ptac* promoter are shown.

955 B. Growth curves of *Azoarcus* sp. CIB (pIZPHTRAP) (filled circles) and *Azoarcus* sp. CIB
956 (pIZPHTRAPΔphtDa) (open triangles). Cells were grown anaerobically on MC minimal

957 medium containing 3 mM PA and 10 mM nitrate as sole donor and electron acceptors,
958 respectively. Gentamicin (7.5 μg ml^{-1}) was added to assure plasmid maintenance.
959 Bacterial growth was monitored by measuring A_{600}.

960 C. Growth curves of *Azoarcus* sp. CIB (pIZPHTRAP) (filled circles) and *Azoarcus* sp. CIB
961 pIZPHTRAPΔphtDa (open triangles) cultivated aerobically on MC minimal medium
962 containing 3 mM PA. Values are the mean of three different experiments. Error bars
963 indicate standard deviations.

964

965

966 **Fig. 4.** Uptake of PA by the PhtTaTb TAXI-TRAP transporter.

967 A. [^{14}C]-PA uptake assays were performed with *Azoarcus* sp. CIB (pIZPHTRAP) cells
968 expressing the PhtTaTb transporter (black bars) and with *Azoarcus* sp. CIB (pIZPHT)
969 control cells that do not express the PhtTaTb transporter (white bars), by using
970 increasing concentrations (5 to 25 μM) of [^{14}C]-PA.

971 B. The uptake rates of [^{14}C]-PA were examined by pre-incubating cells for 10 min with
972 either 1 mM DNP or 1 mM DCCD previous to the transport assay. PA uptake rates were
973 also examined by adding 250 μM non-labelled PA, isophthalate (IPA), or terephthalate
974 (TPA) as competitors to the transport assay containing 25 μM [^{14}C]-PA. Values are the
975 mean of three different experiments. Error bars indicate standard deviations.

976

977 **Fig. 5.** Phylogenetic tree of the solute binding-protein (SBP) of different primary (ABC-
978 type) and secondary (TRAP-, TTT-, TAXI-TRAP-type) transporters of aromatic

compounds. Multiple sequence alignment of the different proteins and the phylogenetic tree were obtained as detailed in Experimental Procedures. The bar represents 0.1 substitutions per amino acid. Protein names, GenBank codes and the name of the microorganism harbouring the corresponding protein are indicated. The substrate of each transporter system is also indicated in parentheses. The prototype SBP of TRAP, TTT and TAXI-TRAP transporters is shown in bold. Among TAXI-TRAP transporters (in blue), the PhtTb protein from *A. aromaticum* EbN1 studied in this work is indicated with an arrow. Orange shadowed are PhtTb-like proteins present in *pht* clusters; yellow shadowed are predicted PhtTb-like proteins present in putative clusters for PA degradation via classical aerobic degradation pathways.

Fig. 6. Expressing the *pht* cassette in *C. necator* H16 cells.

A. Scheme of the putative PA degradation pathways in *C. necator* H16 cells expressing the Pht enzymes that converts PA to benzoyl-CoA. The aerobic hybrid pathway (box pathway) and the classical aerobic pathway (ben-cat pathway) are indicated in blue and red, respectively. Main enzymes and intermediates are shown. Discontinuous arrows indicate that more than one enzymatic step is involved.

B. Growth curves of *C. necator* H16 cells (black line) and *C. necator* H16 (pIZPHTRAP) (green line) on MC minimal medium containing 3 mM PA. Bacterial growth was monitored by measuring A_{600}. Consumption of PA is also indicated (orange line). Values are the mean of three different experiments. Error bars indicate standard deviations.
C. Organization of the *ben-cat* cluster and the two *box* clusters in the genome of strain H16. The *benA*, *boxB*$_1$ and *boxB*$_2$ genes used as probes for monitoring the expression of

1002 the *ben-cat*, *box1* and *box2* clusters, are highlighted. Black arrows show the regulatory
1003 genes.

1004 D. Expression of the *benA*, *boxB*$_1$ and *boxB*$_2$ genes when *C. necator* H16 (pIZPHTRAP)
1005 cells are grown aerobically on 18 mM pyruvate or 3 mM PA. Total RNA was isolated
1006 and the expression of the genes was measured by real-time RT-PCR. The relative
1007 expression of the genes is shown in arbitrary units (AU), being 100 the expression level
1008 of the housekeeping *recA* gene. Each value is the average from three separate
1009 experiments; error bars indicate standard deviations.

1010

1011 **Fig. 7.** Funnelling PA towards the synthesis of PHB in biocatalysts expressing the *pht*
1012 cassette.

1013 A. Scheme of the metabolic pathways involved in the aerobic (white arrows) and
1014 anaerobic (black arrows) conversion of PA to PHB. Abbreviations: Pht, Pht peripheral
1015 pathway; Box, hybrid aerobic pathway; Bzd, anaerobic benzoyl-CoA central
1016 degradation pathway; Pim-Gcd, benzoyl-CoA lower pathway; PhaAB, enzymes involved
1017 in the conversion of acetyl-CoA into the monomeric precursor of PHB, i.e., 3-
1018 hydroxybutyryl-CoA. PhaC, PHB synthase.

1019 B. Representative transmission electron microscopy (TEM) view of *C. necator* H16
1020 (pIZPHTRAP) cells grown aerobically on 3 mM PA. PHB granules can be observed as
1021 white spheres inside the cells.

1022

1023

Table 1. Bacterial strains and plasmids used in this work.

Strains	Relevant genotype and main characteristics[a]	Reference or source
E. coli strains		
DH10B	*F´, mcrA, Δ(mrr hsdRMS-mcrBC), Φ80lacZΔM15, ΔlacX74, deoR, recA1, araD139, Δ(ara-leu)7697, galU, galK, rpsL* (Sm^r)*, endA1, nupG*	Life Technologies
S17-1λ*pir*	Tp^r Sm^r *recA thi hsdRM*$^+$ RP42::.Tc::Mu::Km Tn*7* *λpir* phage lysogen	de Lorenzo and Timmis, 1994
Azoarcus/Aromatoleum strains		
Azoarcus sp. CIB	Wild-type CIB strain, PA^-	López-Barragán *et al.*, 2004
Aromatoleum evansii	Wild-type strain, PA^+	Anders *et al.*, 1995
Cupriavidus strains		
Cupriavidus necator H16	Wild-type strain, PA^-	Pohlmann *et al.*, 2006
Cupriavidus pinatubonensis JMP134	Wild-type strain, PA^-	Don and Pemberton, 1981
Pseudomonas strains		
Pseudomonas putida KT2440	Wild-type strain, PA^-	Franklin *et al.,* 1981

Plasmids		
pIZ1016	Gm^r, pBBR1MCS-5 broad-host range cloning vector	Moreno-Ruiz *et al.*, 2003
pIZPHT	Gm^r, pIZ1016 derivative harbouring the catabolic *pht* genes for the peripheral PA degradation pathway from *Aromatoleum aromaticum* EbN1 strain.	This work
pIZPHTRAP	Gm^r, pIZ1016 derivative harbouring the *pht* cassette for the peripheral PA degradation pathway	This work
pIZPHTRAPΔphtDa	Gm^r, pIZPHTRAP derivative lacking the *phtDa* gene encoding the PCD decarboxylase.	This work

a. The abbreviations used are as follows: Sm^r, steptomycin-resistant; Gm^r, gentamicin-resistant; PA, *o*-phthalate degradation.

Supporting Information

Table S1. Oligonucleotides used in this work.

Fig. S1. Primary structure of the PhtTa protein showing the predicted hydrophobic transmembrane segments.

A. Transmembrane segments (TM) are indicated with red bars (TM1 to TM10) corresponding to a DctM-like large subunit, blue bars (TM12 to TM15) corresponding to a DctQ-like small subunit, and a green bar (TM11) corresponding to a connecting segment of the DctM-like and DctQ-like domains.

B. Probability of each amino acid of the PhtTa protein to be oriented towards the cytoplasm (blue line), membrane (red line) or periplasm (pink line), according to the prediction based on the use of the TMHMM 2.0 program at the DTU Health Tech

server from Technical University of Denmark (http://www.cbs.dtu.dk/services/TMHMM/).

Fig. S2. Expression of the *boxB* gene in aerobically-grown *Azoarcus* sp. CIB (pIZPHTRAP) cells. Cells were grown under oxic conditions on MC minimal medium with 3 mM benzoate (lane 1), 0.2% pyruvate (lane 2) or 3 mM PA (lane 3) as sole carbon source. Total RNA was isolated from cells grown until the end of the exponential phase, and the expression of the *boxB* gene was monitored by RT-PCR. Agarose gel electrophoresis of RT-PCR products is shown. Lane M, molecular size markers (Quick-Load™ 100bp DNA Ladder from New England BioLabs).

Fig. S3. Growth curve of *A. evansii* cultivated aerobically on MC minimal medium containing 3 mM PA as sole carbon source. Bacterial growth was monitored by measuring A_{600}. Values are the mean of three different experiments. Error bars indicate standard deviations.

Fig. S4. Characterization of the composition of the PHB produced by *C. necator* H16 (pIZPHTRAP) cells. Cells were grown aerobically on MC minimal medium with 3 mM benzoate (A) or 3 mM PA (B) as sole carbon source. PHB was isolated, purified and hydrolyzed as detailed in Experimental Procedures. The resulting methyl esters of monomers were anaylzed by GC-MS. The GC chromatograms showing the peaks that correspond to methyl 3-hydroxybutyrate are shown. The insets show the

corresponding mass spectra of the peaks. C. Mass spectrum of standard methyl 3-hydroxybutyrate (NIST Mass Spectrometry Data Center).

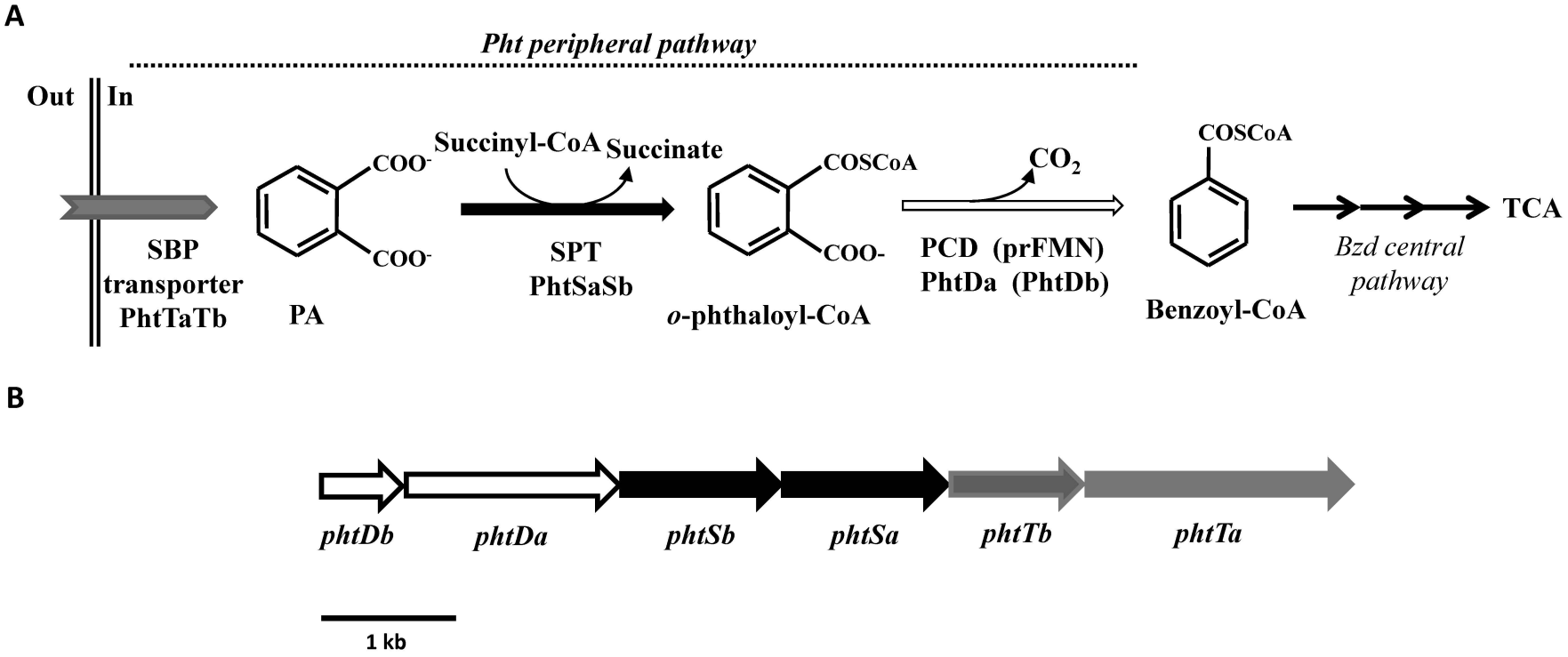
A
Pht peripheral pathway
Out
In
SBP
transporter
PhtTaTb
COO-
COO-
PA
Succinyl-CoA
Succinate
SPT
PhtSaSb
COSCoA
COO-
o-phthaloyl-CoA
CO2
PCD (prFMN)
PhtDa (PhtDb)
COSCoA
Benzoyl-CoA
Bzd central
pathway
TCA
B
phtDb
phtDa
phtSb
phtSa
phtTb
phtTa
1 kb

Fig. 1

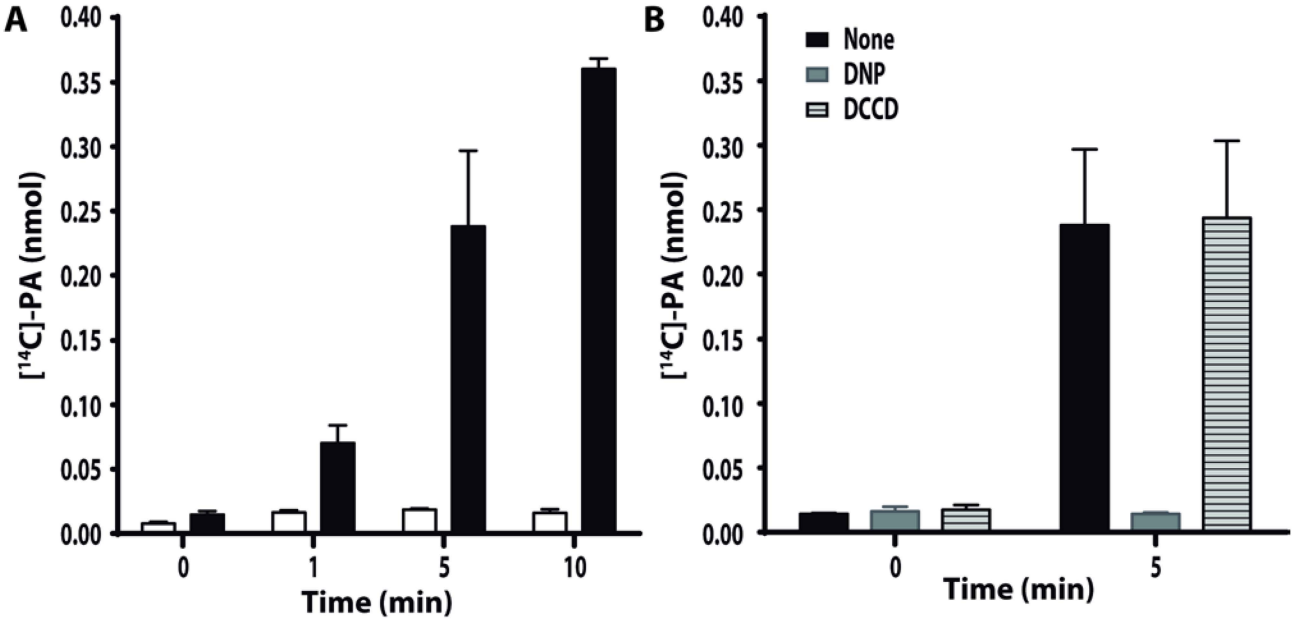
A
B
0.40
0.35
0.30
0.25
0.20
0.15
0.10
0.05
0.00
[14C]-PA (nmol)
0
1
5
10
Time (min)
None
DNP
DCCD
0
5
Time (min)

Fig. 2

A

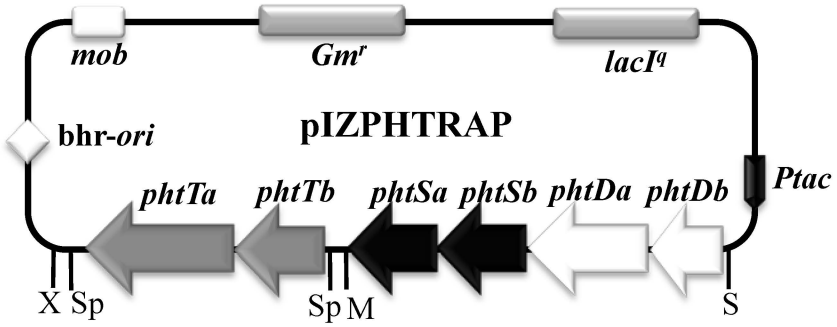
mob
Gm^r
lacI^q
bhr-ori
pIZPHTRAP
phtTa
phtTb
phtSa
phtSb
phtDa
phtDb
Ptac
X Sp
Sp M
S

B

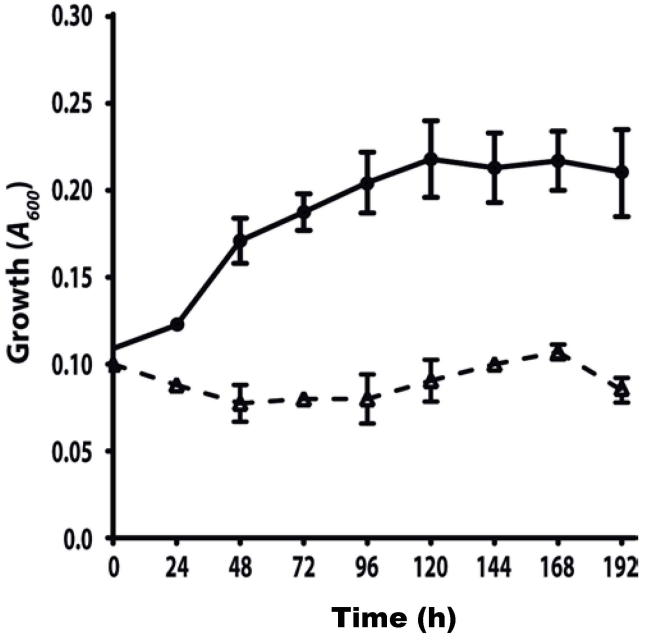
Growth (A_{600})
0.30
0.25
0.20
0.15
0.10
0.05
0.0
0
24
48
72
96
120
144
168
192
Time (h)

C

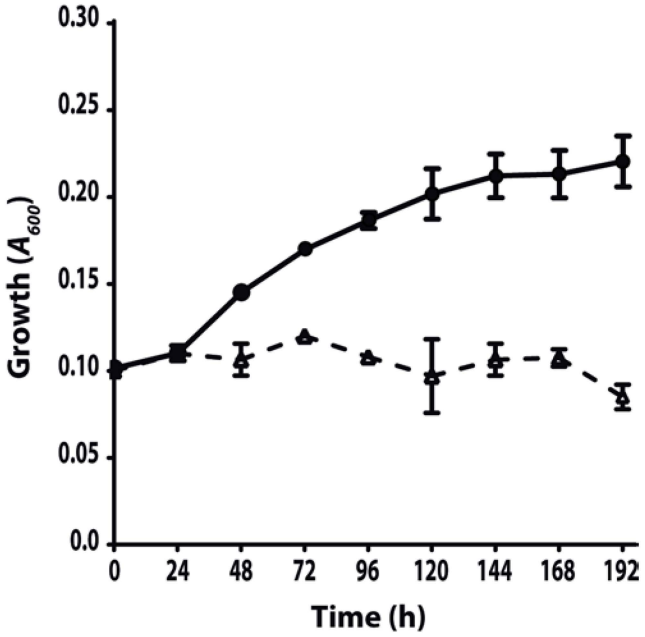
Growth (A_{600})
0.30
0.25
0.20
0.15
0.10
0.05
0.0
0
24
48
72
96
120
144
168
192
Time (h)

Fig. 3

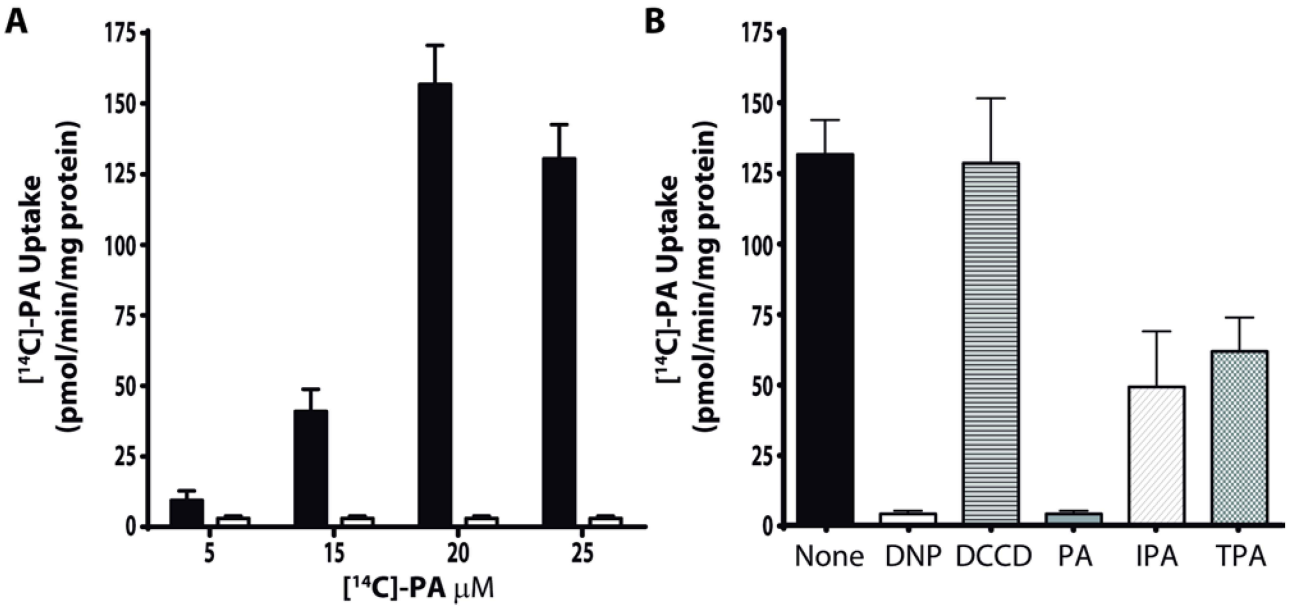
A
[14C]-PA Uptake
(pmol/min/mg protein)
175
150
125
100
75
50
25
0
5
15
20
25
[14C]-PA μM
B
[14C]-PA Uptake
(pmol/min/mg protein)
175
150
125
100
75
50
25
0
None
DNP
DCCD
PA
IPA
TPA

Fig. 4

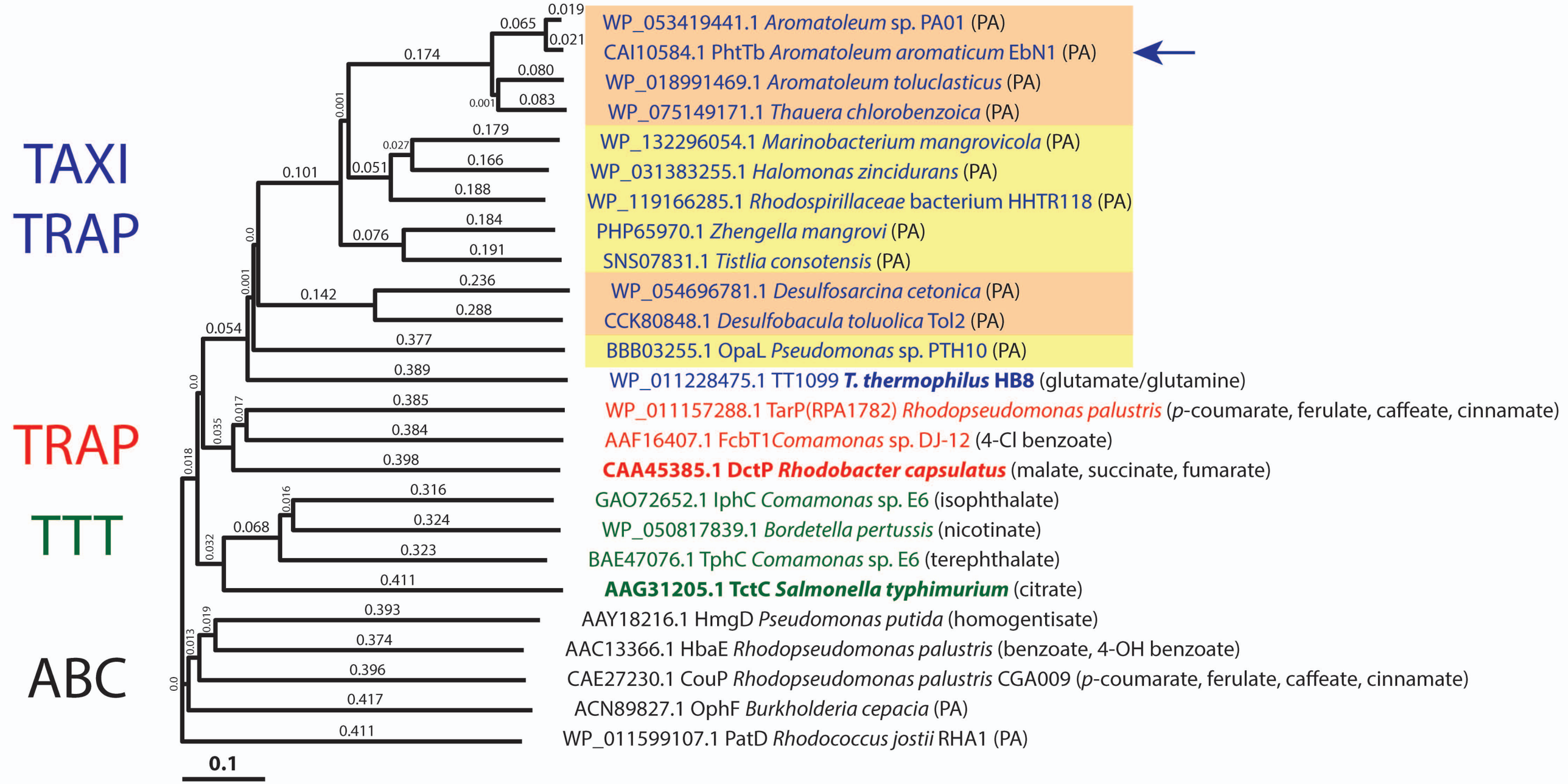
TAXI
TRAP
TRAP
TTT
ABC
0.019
0.065
0.021
0.174
0.080
0.001
0.083
0.001
0.179
0.027
0.166
0.051
0.101
0.188
0.184
0.076
0.191
0.0
0.001
0.236
0.142
0.288
0.054
0.377
0.389
0.0
0.385
0.017
0.035
0.384
0.018
0.398
0.316
0.016
0.324
0.068
0.032
0.323
0.411
0.393
0.019
0.374
0.013
0.396
0.0
0.417
0.411
0.1
WP_053419441.1 Aromatoleum sp. PA01 (PA)
CAI10584.1 PhtTb Aromatoleum aromaticum EbN1 (PA)
WP_018991469.1 Aromatoleum toluclasticus (PA)
WP_075149171.1 Thauera chlorobenzoica (PA)
WP_132296054.1 Marinobacterium mangrovicola (PA)
WP_031383255.1 Halomonas zincidurans (PA)
WP_119166285.1 Rhodospirillaceae bacterium HHTR118 (PA)
PHP65970.1 Zhengella mangrovi (PA)
SNS07831.1 Tistlia consotensis (PA)
WP_054696781.1 Desulfosarcina cetonica (PA)
CCK80848.1 Desulfobacula toluolica Tol2 (PA)
BBB03255.1 OpaL Pseudomonas sp. PTH10 (PA)
WP_011228475.1 TT1099 T. thermophilus HB8 (glutamate/glutamine)
WP_011157288.1 TarP(RPA1782) Rhodopseudomonas palustris (p-coumarate, ferulate, caffeate, cinnamate)
AAF16407.1 FcbT1Comamonas sp. DJ-12 (4-Cl benzoate)
CAA45385.1 DctP Rhodobacter capsulatus (malate, succinate, fumarate)
GAO72652.1 IphC Comamonas sp. E6 (isophthalate)
WP_050817839.1 Bordetella pertussis (nicotinate)
BAE47076.1 TphC Comamonas sp. E6 (terephthalate)
AAG31205.1 TctC Salmonella typhimurium (citrate)
AAY18216.1 HmgD Pseudomonas putida (homogentisate)
AAC13366.1 HbaE Rhodopseudomonas palustris (benzoate, 4-OH benzoate)
CAE27230.1 CouP Rhodopseudomonas palustris CGA009 (p-coumarate, ferulate, caffeate, cinnamate)
ACN89827.1 OphF Burkholderia cepacia (PA)
WP_011599107.1 PatD Rhodococcus jostii RHA1 (PA)

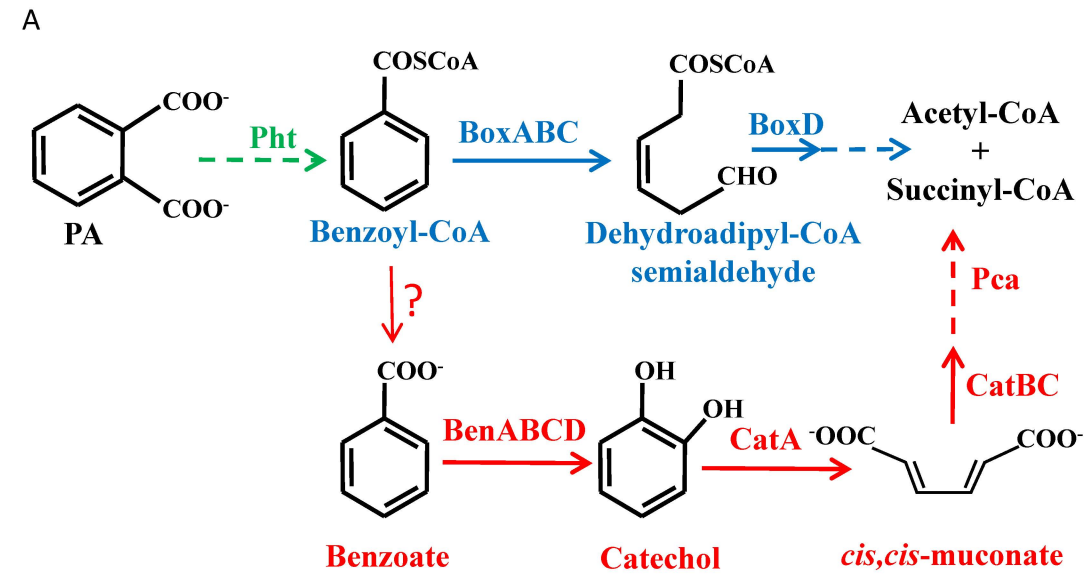
A
COO-
COO-
PA
Pht
COSCoA
Benzoyl-CoA
BoxABC
COSCoA
CHO
Dehydroadipyl-CoA
semialdehyde
BoxD
Acetyl-CoA
+
Succinyl-CoA
Pca
CatBC
?
COO-
Benzoate
BenABCD
OH
OH
Catechol
CatA
-OOC
COO-
cis,cis-muconate

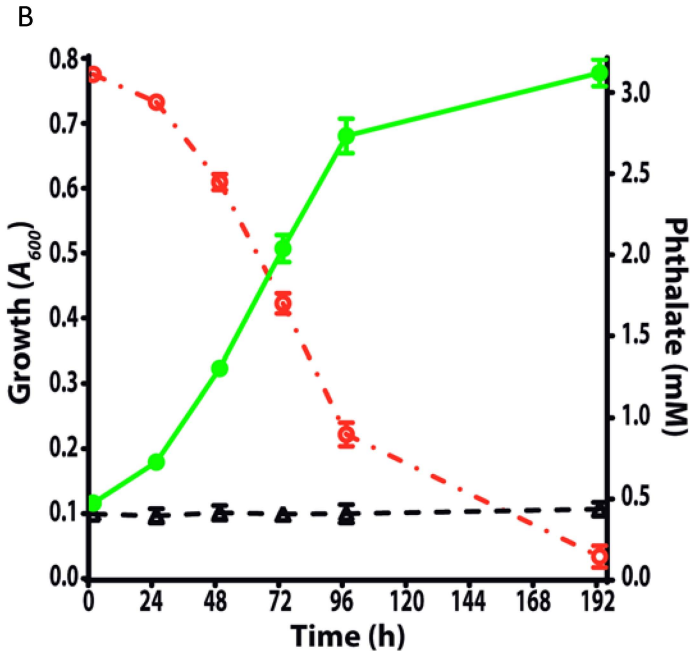
B
Growth (A_{600})
Phthalate (mM)
Time (h)
0.0
0.1
0.2
0.3
0.4
0.5
0.6
0.7
0.8
0.0
0.5
1.0
1.5
2.0
2.5
3.0
0
24
48
72
96
120
144
168
192

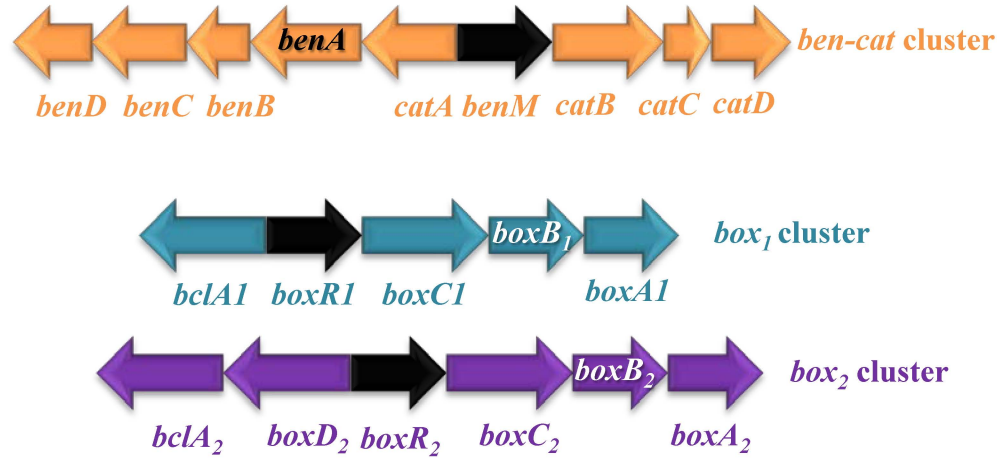
C
benA
ben-cat cluster
benD benC benB
catA benM catB catC catD
boxB1
box1 cluster
bclA1 boxR1 boxC1
boxA1
boxB2
box2 cluster
bclA2 boxD2 boxR2 boxC2
boxA2

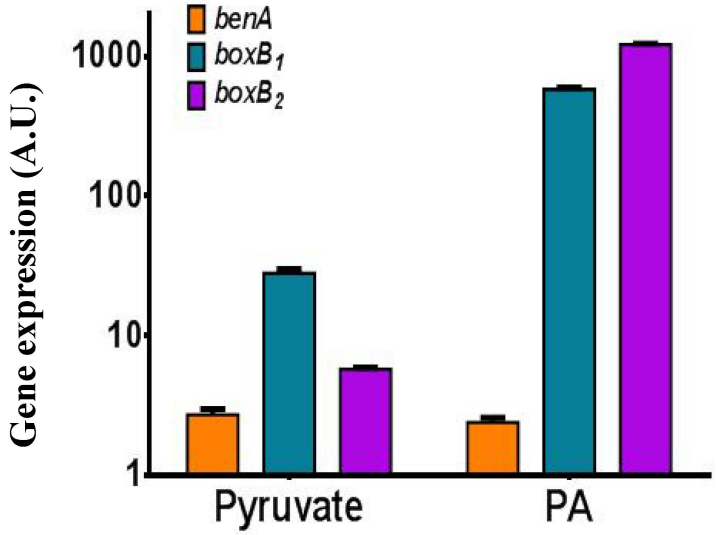
D
benA
boxB1
boxB2
Gene expression (A.U.)
1000
100
10
1
Pyruvate
PA

Fig. 6

A

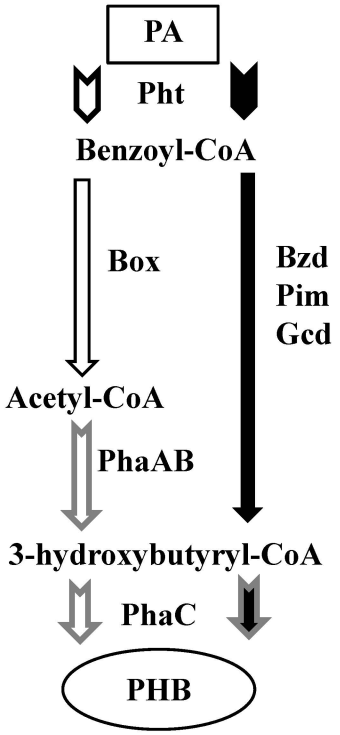
PA
Pht
Benzoyl-CoA
Box
Bzd
Pim
Gcd
Acetyl-CoA
PhaAB
3-hydroxybutyryl-CoA
PhaC
PHB

B

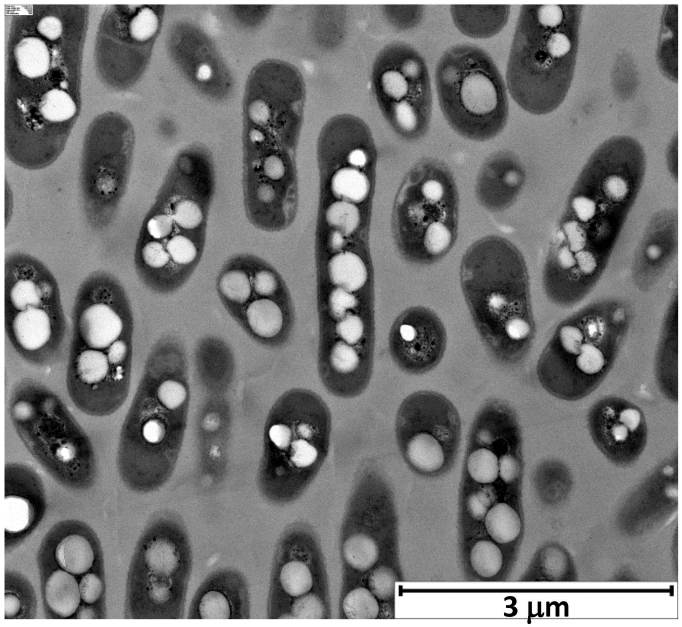
3 µm

Fig. 7